Pho4 mediates phosphate acquisition in *Candida albicans* and is vital for stress resistance and metal homeostasis

Mélanie A. C. Ikeh[a,†], Stavroula L. Kastora[b], Alison M. Day[a], Carmen M. Herrero-de-Dios[b], Emma Tarrant[a], Kevin J. Waldron[a], A. Peter Banks[a], Judith M. Bain[b], David Lydall[a], Elizabeth A. Veal[a], Donna M. MacCallum[b], Lars P. Erwig[b], Alistair J. P. Brown[b], and Janet Quinn[a,*]
[a]Institute for Cell and Molecular Biosciences, Faculty of Medical Sciences, Newcastle University, Newcastle upon Tyne NE2 4HH, United Kingdom; [b]School of Medical Sciences, University of Aberdeen, Aberdeen AB25 2ZD, United Kingdom

ABSTRACT During interactions with its mammalian host, the pathogenic yeast *Candida albicans* is exposed to a range of stresses such as superoxide radicals and cationic fluxes. Unexpectedly, a nonbiased screen of transcription factor deletion mutants revealed that the phosphate-responsive transcription factor Pho4 is vital for the resistance of *C. albicans* to these diverse stresses. RNA-Seq analysis indicated that Pho4 does not induce stress-protective genes directly. Instead, we show that loss of Pho4 affects metal cation toxicity, accumulation, and bioavailability. We demonstrate that *pho4Δ* cells are sensitive to metal and nonmetal cations and that Pho4-mediated polyphosphate synthesis mediates manganese resistance. Significantly, we show that Pho4 is important for mediating copper bioavailability to support the activity of the copper/zinc superoxide dismutase Sod1 and that loss of Sod1 activity contributes to the superoxide sensitivity of *pho4Δ* cells. Consistent with the key role of fungal stress responses in countering host phagocytic defenses, we also report that *C. albicans pho4Δ* cells are acutely sensitive to macrophage-mediated killing and display attenuated virulence in animal infection models. The novel connections between phosphate metabolism, metal homeostasis, and superoxide stress resistance presented in this study highlight the importance of metabolic adaptation in promoting *C. albicans* survival in the host.

INTRODUCTION

The fungus *Candida albicans* is a constituent of the normal human microbiome. It resides on the skin, in the oral cavity, and in the gastrointestinal and urogenital tracts of most healthy individuals (Odds, 1988). However, as an opportunistic pathogen, this fungus is poised to cause superficial infections in otherwise healthy individuals or life-threatening systemic infections in immunocompromised hosts.

Candida species are the fourth-most-common cause of nosocomial bloodstream infections (Wisplinghoff *et al.*, 2004), and estimates indicate that *C. albicans* is responsible for ~400,000 systemic infections per year (Brown *et al.*, 2012). Such infections, which are associated with alarming crude mortality rates of >40%, occur after entry of the fungus into the bloodstream, followed by dissemination to internal organs such as the kidney, liver, and brain (Morgan, 2005). Therefore *C. albicans* can colonize diverse anatomical sites of the human host, demonstrating its significant capacity to adapt to contrasting environments.

A major factor underlying this adaptability is the ability of *C. albicans* to rapidly mount transcriptional responses after exposure to host-imposed stresses (for a review, see Wilson *et al.*, 2009). For example, consistent with neutrophils and macrophages producing high levels of reactive oxygen species (ROS), genome-wide profiling has revealed that *C. albicans* induces many oxidative stress–responsive genes after phagocytosis (Fradin *et al.*, 2003, 2005; Rubin-Bejerano *et al.*, 2003; Lorenz *et al.*, 2004; Enjalbert *et al.*, 2007). During invasion of the liver, a number of pH-responsive genes and heat shock

proteins, together with genes encoding transporters for vital micronutrients, including iron and phosphate, are induced (Thewes et al., 2007). In a mucosal infection model of oral candidiasis, the fungus up-regulates nitrosative stress-responsive genes, as well as genes indicating that *C. albicans* also faces a nitrogen-, glucose-, and phosphate-poor environment in the oral tissue (Zakikhany et al., 2007). Such genome-wide profiling studies, which have captured the transcriptional response of *C. albicans* in different infection models, provide significant insight into the particular stresses encountered by this pathogen when colonizing specific host environments.

The ability of *C. albicans* to mount such stress responses within different host niches is essential for virulence (for a review, see Brown et al., 2014b). For example, the inactivation of genes that are induced in the host and encode enzymes that detoxify ROS (catalase, Cat1; superoxide dismutases, Sod1, Sod5; thioredoxin, Trx1; glutaredoxin, Grx2) or reactive nitrogen species (the hemoprotein Yhb1) attenuates the virulence of *C. albicans* in mouse models of systemic candidiasis (Wysong et al., 1998; Hwang et al., 2002; Martchenko et al., 2004; Hromatka et al., 2005; Chaves et al., 2007; da Silva Dantas et al., 2010). In addition, mutants lacking the Hog1 stress-activated protein kinase, which plays key roles in stress signaling and stress-responsive gene expression, display impaired virulence in multiple infection models (Alonso-Monge et al., 1999; Prieto et al., 2014). The ability to acquire essential nutrients is also vital for *C. albicans* to colonize nutrient-poor environments within the host (Brown et al., 2014a). For example, *C. albicans* cells lacking Pga7 or Pra1, which play major roles in the scavenging of iron and zinc, respectively, exhibit reduced virulence (Kuznets et al., 2014).

Although adaptation to host niches and virulence are intimately linked, there is still much to be learned about the mechanisms underlying the adaptability of *C. albicans* to the diverse environments encountered within the host. After phagocytosis, microbes are exposed to high levels of superoxide anions generated by the respiratory burst (Reeves et al., 2002). The resulting accumulation of anionic charge is compensated by a rush of potassium (K^+) ions into the endocytic vacuole, which also imposes a cationic stress on the microbe (Reeves et al., 2002). However, we know little regarding the transcriptional regulators required for *C. albicans* resistance to these phagocyte-imposed stresses. Here we performed a nonbiased screen of transcription factor deletion mutants to identify the Pho4 transcription factor as being essential for resistance to both superoxide and cationic stresses in *C. albicans*. We find that Pho4 is an important virulence determinant in *C. albicans*, consistent with stress adaptation being vital for fungal pathogenesis. However, rather than Pho4 directly regulating the expression of stress-protective genes, we provide evidence that many of the stress phenotypes exhibited by *pho4Δ* cells relate to effects on metal homeostasis.

RESULTS

Cells lacking *PHO4* display pleiotropic stress phenotypes

To identify transcription factors that promote resistance to cationic stress or superoxide stress, we screened a *C. albicans* transcription factor deletion library (Homann et al., 2009) for mutants that display impaired fitness compared with wild-type cells upon exposure to NaCl (1 M) or the superoxide-generating drug menadione (300 μM). Strain fitness was measured by quantitative fitness analysis (QFA), in which liquid cultures of exponentially growing cells were spotted onto solid agar and growth monitored by time-course photography. Images were processed and quantitative growth parameters determined using Colonyzer software (Lawless et al., 2010), allowing for the generation of fitness plots (Figure 1, A and B). Deviations from wild-type fitness generated a stress interaction score (SIS), with the

lowest SIS indicative of most-impaired fitness. The SIS of all mutants after exposure to NaCl or menadione stress is listed in Supplemental Table S1. More mutants showed impaired fitness to menadione-induced superoxide stress than to cationic stress. The 10 strains with the greatest impairment of resistance to these stress conditions are highlighted in red in Figure 1, A and B, and listed in Table 1.

Three transcription factors listed in Table 1 are required for optimal fitness in response to both cationic and superoxide stress: Pho4, Efg1, and Rim101. Efg1 has well-characterized roles in regulating hyphal growth (Stoldt et al., 1997), whereas Rim101 is important for the alkaline pH response (Davis et al., 2000). Previous phenotypic profiling showed that Rim101 was important for resistance to the cationic stress–inducing agent LiCl, and cells lacking Efg1 or Rim101 were shown to display marginal sensitivity to menadione (Homann et al., 2009). In contrast, the cationic and menadione stress–protective roles of Pho4 have not previously been reported in *C. albicans*. Here it is noteworthy that in the original phenotypic screen of the transcription factor deletion collection (Homann et al., 2009), a lower concentration of menadione (90 μM) was used than in this study (300 μM). This likely underlies why, in the original screen, *pho4Δ* cells were not designated as menadione sensitive (Homann et al., 2009). The analogous Pho4 transcription factor in *Saccharomyces cerevisiae* plays vital roles in phosphate acquisition and storage (Ogawa et al., 2000), and although it is required for growth under alkaline pH conditions (Sambade et al., 2005), cationic and oxidative stress-sensitive phenotypes have not been reported. On the basis of these observations, we decided to investigate further the stress-protective roles of the Pho4 transcription factor in *C. albicans*.

The stress sensitivities of the *pho4Δ* mutant were confirmed in spot-test experiments. The *pho4Δ* cells were more sensitive than wild-type cells to cationic and superoxide stresses imposed by NaCl and menadione, respectively, and these stress phenotypes were rescued upon reintegration of the *PHO4* gene (Figure 1C). We also noted that *pho4Δ* cells grew more slowly than wild-type cells on rich medium (Figure 1C). Cells lacking *PHO4* were not sensitive to sorbitol, indicating a cation-specific rather than an osmotic stress–protective role (Figure 1C). In addition, *pho4Δ* cells were not notably sensitive to hydrogen peroxide, suggesting that Pho4 plays a specific role in superoxide protection (Figure 1C). Pho4 was also vital for the growth of *C. albicans* cells under alkaline but not acidic pH environments (Figure 1C), similar to that reported in *S. cerevisiae* (Sambade et al., 2005). Related to the neutral/alkaline pH of serum, the growth of cells lacking *PHO4* was also impaired on medium containing serum (Figure 1D), and serum-induced filamentation was significantly delayed (Figure 1D).

C. albicans Pho4 is required for phosphate acquisition and storage

In *S. cerevisiae*, the Pho4 transcription factor plays a central role in phosphate acquisition when extracellular inorganic phosphate (P_i) concentrations are low. In P_i-rich environments Pho4 is phosphorylated by the Pho85-Pho80 cyclin-dependent protein kinase (CDK) complex, which prevents its nuclear accumulation (Schneider et al., 1994; O'Neill et al., 1996). However, when P_i levels are limiting, the Pho85-Pho80 CDK is inhibited via the action of the Pho81 CDK inhibitor, and the resulting unphosphorylated Pho4 accumulates in the nucleus. Subsequently Pho4 induces genes encoding proteins involved in phosphate acquisition and in the synthesis of the phosphate storage molecule polyphosphate (polyP; Ogawa et al., 2000). However, sequence homology between the *S. cerevisiae* and *C. albicans* Pho4 transcription factors is largely restricted to the C-terminal
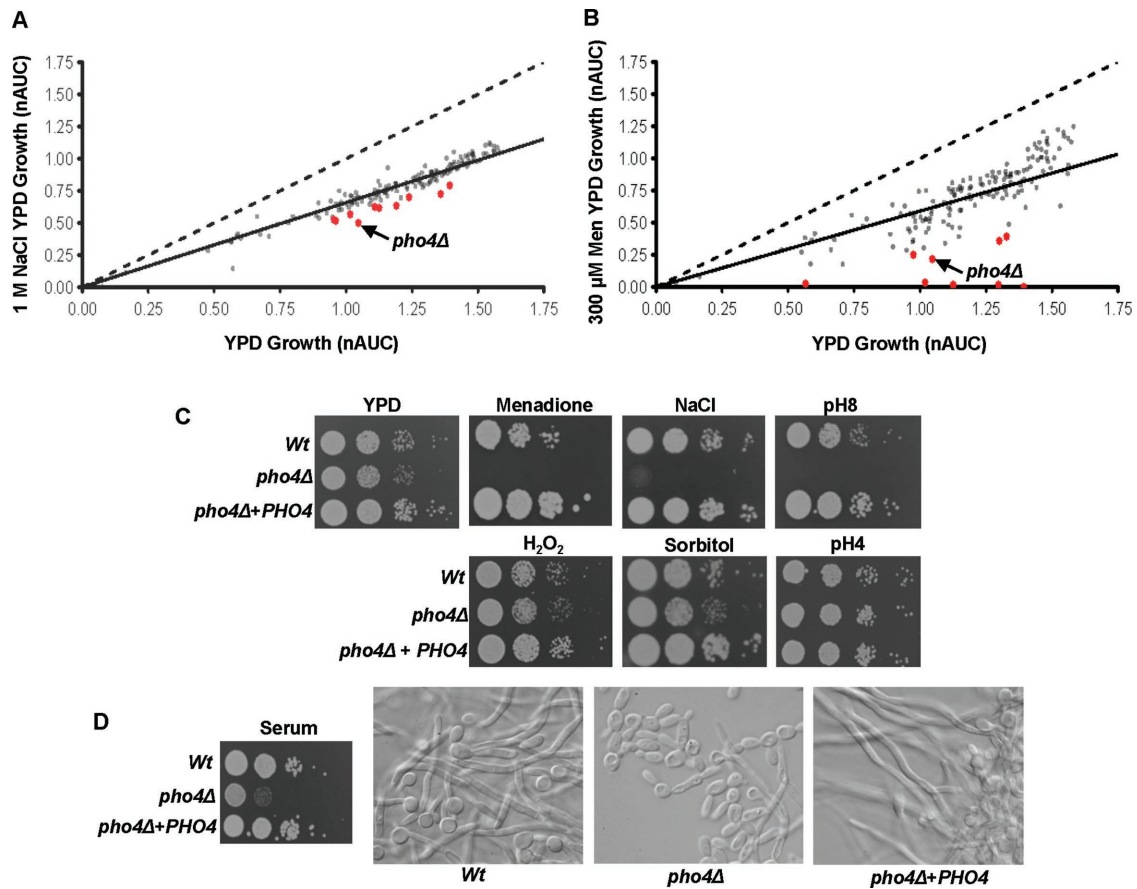
FIGURE 1: Cells lacking *PHO4* display pleiotropic stress phenotypes. Quantitative fitness analysis plot of the transcription factor deletion library grown on media containing (A) 1 M NaCl and (B) 300 µM menadione. The line of equal growth (dashed line) and a multiplicative model of expected fitness (solid line) are indicated. The top 10 sensitive strains are indicated by red dots. (C) Exponentially growing strains were spotted in serial dilutions onto YPD plates containing 1 M NaCl, 300 µM menadione, 1.2 M sorbitol, or 5 mM H_2O_2. The pH of YPD was adjusted using 1 M Tris-HCl (pH 8.25) for pH 8 medium and 1 M succinic acid for pH 4 medium. Plates were incubated for 24 h at 30°C. (D) *pho4Δ* cells are sensitive to serum and display delayed serum-induced hyphal growth. Exponentially growing strains were spotted onto YPD plates containing 20% fetal bovine serum (left), or stationary-phase cells were diluted 1:10 in YPD medium containing 10% fetal bovine serum and incubated at 37°C for 4 h (right).

Systematic name	Standard name	SIS NaCl	Systematic name	Standard name	SIS Men
C4_05680W_A	***PHO4***	−0.19437	CR_07890W_A	***EFG1***	−0.82282
C5_01910W_A	*GIS2*	−0.1752	C7_03220C_A	*ZCF29*	−0.75071
C2_01890W_A	*CTF1*	−0.15782	C3_02220W_A	*CAP1*	−0.66091
CR_07890W_A	***EFG1***	−0.13318	C1_14340C_A	***RIM101***	−0.64918
C1_14340C_A	***RIM101***	−0.12753	C3_02220W_A	*NDT80*	−0.56936
C6_00280W_A	*CPH2*	−0.11684	C1_04330W_A	*RPN4*	−0.40951
C2_10540W_A	*C2_10540W_A*	−0.11612	C4_05680W_A	***PHO4***	−0.40382
C4_05700W_A	*ZCF5*	−0.10933	C5_00240W_A	*SKN7*	−0.39617
C3_05470W_A	*TEA1*	−0.10644	C2_00430C_A	*DPB4*	−0.33
C3_06310C_A	*ISW2*	−0.10241	C5_01810W_A	*FCR3*	−0.30926

Mutants sensitive to both stresses are indicated in bold.

TABLE 1: Stress interaction scores (SIS) of 10 most sensitive transcription factor deletion mutants to cationic (NaCl) and superoxide (menadione [Men]) stress.
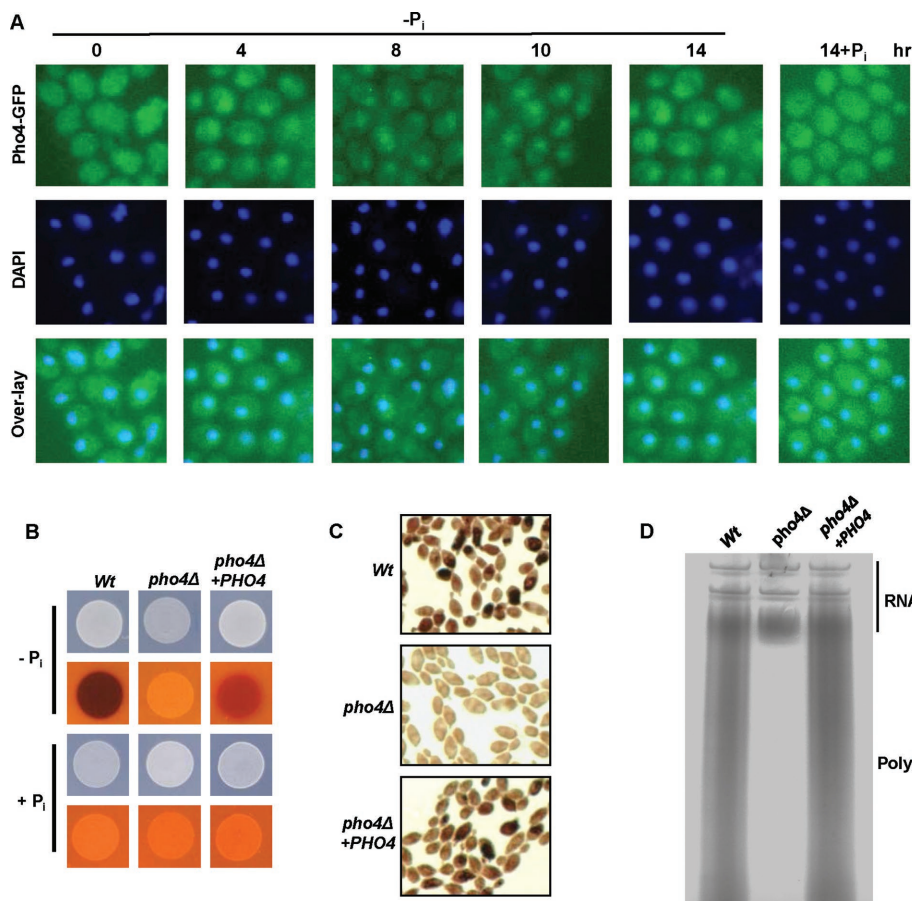
FIGURE 2: Cells lacking *PHO4* cannot acquire or store phosphate. (A) Pho4 accumulates in the nucleus under phosphate-limiting conditions. Cells expressing Pho4-GFP were transferred to YPD medium lacking phosphate, and localization was determined by fluorescence microscopy over a 14-h time course. +P_i indicates phosphate addition (10 min) to the 14-h sample. DAPI staining illustrates nuclear positioning. (B) Under phosphate-limiting conditions, Pho4 is required for acid phosphatase activity. Strains grown on PNMC agar plates with or without P_i were subjected to an agar-overlay coloration assay in which secreted acid phosphatase activity is visualized by a dark red coloration. (C, D) Pho4 is required for the storage of P_i as polyphosphate. Visualization of polyphosphate by (C) Neisser staining of cells and (D) toluidine blue staining of RNA/polyP extracts after electrophoresis on urea-polyacrylamide gels.

pink color. *C. albicans* Pho4 was found to be critical for polyP accumulation, as revealed both by Neisser staining of whole cells (Figure 2C) and toluidine blue staining of polyP resolved on polyacrylamide gels (Figure 2D). Thus, despite sequence differences with its *S. cerevisiae* orthologue, the *C. albicans* Pho4 transcription factor is responsive to P_i-limiting environments and plays key roles in phosphate accumulation and storage.

polyP is not required for Pho4-mediated stress resistance

Pho4 in *C. albicans* is required for resistance to a range of distinct stress conditions (Figure 1) in addition to phosphate uptake and storage (Figure 2). Therefore we asked whether Pho4 played a direct role in stress-protective gene expression or whether the stress phenotypes displayed by *pho4Δ* cells were due to the role of Pho4 in phosphate acquisition. Initially, we examined whether Pho4 accumulated in the nucleus after cationic, superoxide, and alkaline pH stresses, similar to what occurs in P_i-limiting environments. Pho4 rapidly accumulated in the nucleus after alkaline pH stress, but we could not detect changes in the cellular localization of Pho4 after cationic or superoxide stress (Figure 3A). The lack of nuclear accumulation after cationic or superoxide stress suggested that Pho4 might play an indirect, nontranscriptional role in mediating resistance to these stresses. Related to this, the phosphate storage molecule polyP has been implicated in stress adaptation and osmoregulation in bacteria and lower eukaryotic species, such as yeast, fungi, and trypanosomes (reviewed in Moreno and Docampo, 2013). Hence we investigated whether polyP synthesis was a key determinant in mediating Pho4-dependent stress resistance. Initially, we examined whether polyP was mobilized after exposure to different stresses. Neisser staining and gel electrophoresis revealed that there was a drastic decrease in polyP levels 10 h after transferring cells from P_i-replete to P_i-limiting medium (Figure 3, B and C). No obvious differences were observed after superoxide stress (Figure 3B and Supplemental Figure S1). A rapid decrease in polyP levels was observed, however, after alkaline pH stress and, to some extent, cationic stress (Figure 3, B–D). This suggested that perhaps the role of Pho4 in mediating resistance to alkaline and cationic stresses was due to its role in polyP production.

To examine this directly, we tested whether the physical presence of polyP was important for stress resistance in *C. albicans*. In *S. cerevisiae*, polyP synthesis is dependent on the yeast vacuolar transporter chaperone (VTC) complex, which is a membrane protein assembly comprising the Vtc1-4 proteins (Figure 4A). Vtc4 has been identified as the polyP polymerase within the VTC complex (Hothorn et al., 2009), and *S. cerevisiae vtc4Δ* and *vtc1Δ* null mutants lack detectable polyP (Ogawa et al., 2000; Hothorn et al., 2009). Hence we generated *C. albicans* strains lacking homologues of the *VTC1*

DNA-binding domain (Urrialde *et al.*, 2015), and key phosphorylation sites implicated in Pho4 regulation in *S. cerevisiae* do not appear to be conserved in *C. albicans* Pho4. Therefore we ascertained whether the function of Pho4 in phosphate accumulation and storage is conserved in *C. albicans*.

We created a *C. albicans* strain expressing Pho4-GFP and examined the cellular localization of Pho4. Pho4 gradually accumulates in the nucleus after growth in P_i-limiting medium, and this is rapidly reversed after addition of phosphate (Figure 2A). *C. albicans* also responds to phosphate limitation by increasing the level of secreted acid phosphatase activity in a Pho4-dependent manner (Figure 2B). We examined the role of Pho4 in polyP accumulation using two different techniques to visualize polyP. Neisser staining is routinely used to detect polyP in whole cells and uses a basic methylene blue dye that stains the polyP granules metachromatically a purple/black color (Gurr, 1965). A second method involves electrophoresis of polyP extracted from cells on urea-polyacrylamide gels, followed by staining with a different basic dye, toluidine blue (Smith and Morrissey, 2007). Toluidine blue staining of polyP results in a metachromatic shift in the absorption spectrum of this dye to give a purple/
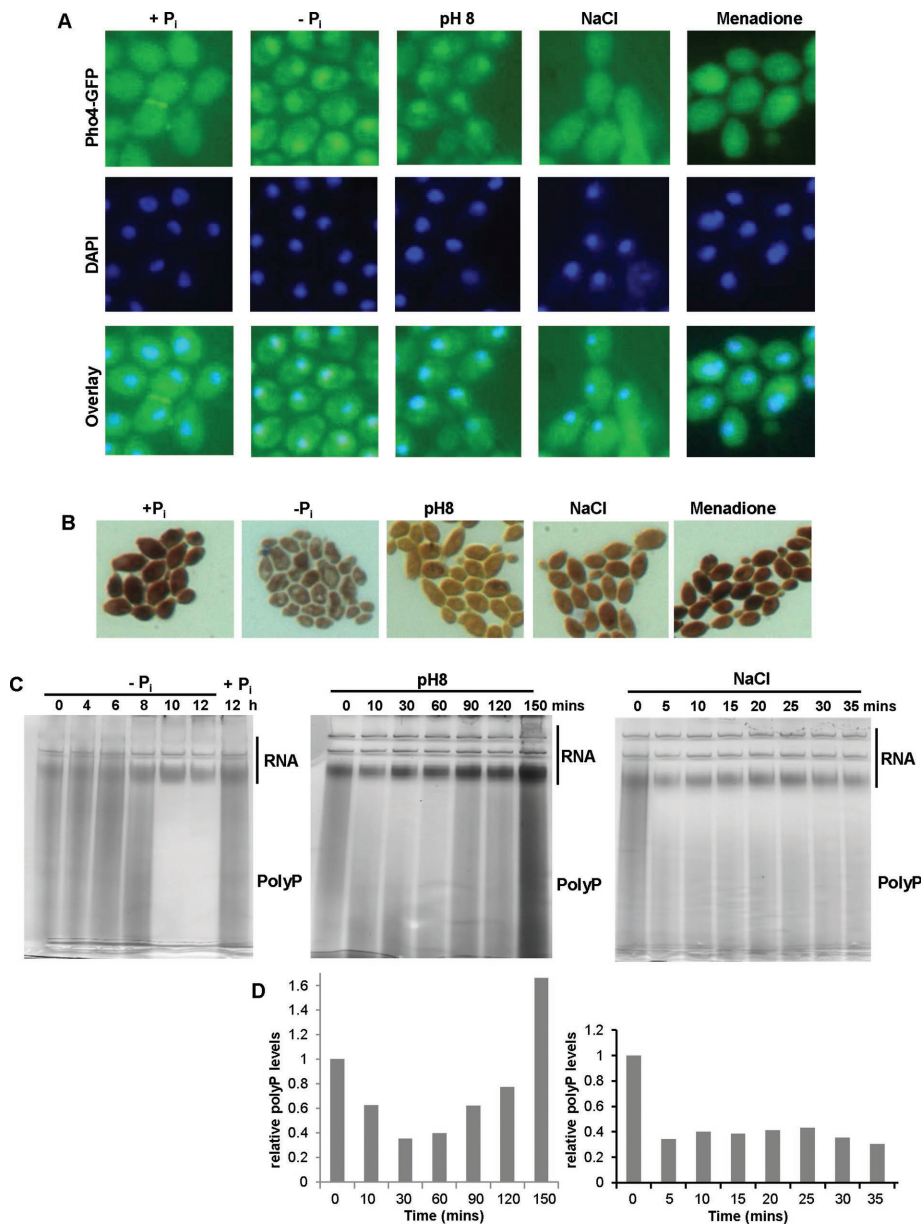
FIGURE 3: Pho4 localization and polyP mobilization in response to specific stress treatments. (A) Pho4 accumulates in the nucleus only after P$_i$ limitation or exposure to alkaline pH. *C. albicans* cells expressing Pho4-GFP were grown in YPD –P$_i$ (10 h) or YPD pH 8 (10 min) or exposed to 1 M NaCl (10 min) or 300 µM menadione (10 min), and Pho4 localization was imaged using fluorescence microscopy. DAPI staining illustrates nuclear positioning. (B, C) PolyP is mobilized in response to specific stresses. (B) Neisser staining of cells treated as described in A. (C) Toluidine blue staining of RNA/polyP extracts after electrophoresis on urea-polyacrylamide gels from cells grown in YPD –P$_i$, YPD pH 8, or YPD containing 1 M NaCl for the indicated times. (D) The amount of polyphosphate after exposure to pH 8 or 1 M NaCl normalized to the amount of RNA loaded on the gel.

cells (Figure 4D), indicating the presence of additional genome changes during strain construction. Nonetheless, these results indicate that the drastic reduction of polyP levels in *pho4Δ* cells does not underlie the phenotypes associated with loss of Pho4.

RNA-sequencing analysis defines the Pho4-regulon

Although the lack of nuclear accumulation of Pho4 after cationic and superoxide stress (Figure 3A) suggested that this transcription factor might not directly regulate stress-protective genes, we reasoned that the identification of the Pho4-regulon in *C. albicans* might provide insight into the mechanism underlying the stress-protective roles of this transcription factor. To this end, we used RNA-sequencing (RNA-Seq) analysis to compare the transcription profiles of wild-type and *pho4Δ* null cells under both phosphate-replete (+P$_i$) and phosphate-limiting (–P$_i$) conditions. We grew cells in phosphate-limiting medium for 16 h and then harvested them (–P$_i$ samples). For the +P$_i$ samples, we subsequently added 10 mM phosphate to the phosphate-starved cultures and harvested samples 2 h later. We analyzed three independent replicates for each condition and validated the RNA-Seq output by targeted analysis of specific transcripts (described later). The complete data set is presented in Supplemental Table S2.

Figure 5A shows heat maps depicting *C. albicans* gene regulation in response to phosphate limitation and *PHO4* deletion. Genes that displayed a twofold or smaller decrease in transcript levels in *pho4Δ* cells in comparison to wild-type cells were classified as Pho4-dependent targets. From this analysis, 822 genes were found to be significantly up-regulated in wild-type cells in phosphate-limiting medium compared with phosphate-replete conditions. Of these, 150 displayed Pho4 dependence for their induction (see Supplemental Table S2 for the full data set). We constructed a Cytoscape network that illustrates the functional categories (Gene Ontology [GO] terms) that are significantly enriched in the subset of *C. albicans* genes induced in wild-type cells under phosphate-limiting conditions and the contribution of Pho4 to

and *VTC4* polyP synthesis genes and explored polyP levels and stress resistance phenotypes of these mutants. PolyP levels were markedly reduced in cells lacking *VTC1* or *VTC4* (Figure 4, B and C). Phenotypic analyses of these mutants, however, revealed no overlap with the cationic, superoxide, and alkaline pH stress–sensitive phenotypes exhibited by *pho4Δ* cells (Figure 4D and Supplemental Figure S2A) or defects in serum-induced filamentation (Supplemental Figure S2B). The *vtc4Δ + VTC4* mutant was unexpectedly but reproducibly slightly more sensitive to menadione than wild-type

these processes (Figure 5B). The following functional categories were significantly enriched: Phosphate Accumulation, Response to Single Organism Metabolic Processes, Cellular Response to Stress, Oxidation/Reduction Processes, and Cellular Response to DNA Damage Stimulus (Figure 5B). Consistent with the phenotypes we observed for *pho4Δ* cells, Pho4 contributes to several of these functional categories, including Phosphate Accumulation, Oxidation/Reduction Processes, and Cellular Response to Stress (Figure 5B).
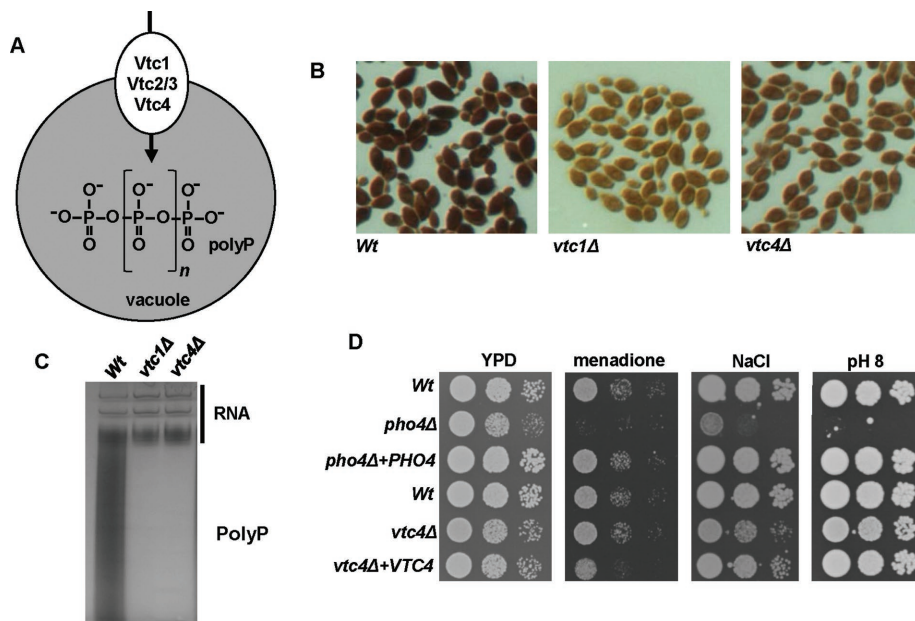
FIGURE 4: PolyP synthesis and effect on *C. albicans* stress resistance. (A) Overview of the proteins involved in polyP synthesis. (B, C) PolyP synthesis is dependent on Vtc1 and Vtc4. (B) Neisser staining of the indicated strains. (C) Toluidine blue staining of RNA/polyP extracts from indicated strains after electrophoresis on urea-polyacrylamide gels. (D) PolyP is dispensable for Pho4-associated stress-sensitive phenotypes. Exponentially growing strains were spotted in serial dilutions onto YPD plates containing 1 M NaCl or 300 μM menadione or onto YPD pH 8. Plates were incubated for 24 h at 30°C.

An examination of genes with predicted roles in phosphate accumulation and storage revealed that Pho4 was required for the expression of the high-affinity phosphate transporter *PHO84*, several acid phosphatase genes (*PHO100*, *PHO112* and *PHO113*), and the *VTC1* and *VTC3* genes implicated in polyphosphate synthesis. The Pho4 dependence of *PHO84* and *PHO100*, which was confirmed by Northern blotting (Figure 5C), is in line with the roles of Pho4 in phosphate sensing and accumulation (Figure 2). In addition, the role of Pho4 in mediating the induction of *VTC1* and *VTC3* is consistent with the lack of polyphosphate in *pho4Δ* cells (Figure 2, C and D). In agreement with previous reports (Bishop *et al.*, 2011, 2013), Pho4 was also required for induction of the *GIT1-3* genes, which encode transporters for glycerophosphodiesters, and the *GDE1* gene, which encodes a glycerophosphocholine phosphodiesterase. Glycerophosphodiesters are products of phospholipase-mediated deacylation of phospholipids and an important source of phosphate in *C. albicans* (Bishop *et al.*, 2011).

Pho4-dependent genes and stress phenotypes

We next explored whether genes deregulated in *pho4Δ* cells under phosphate-limiting conditions could account for the superoxide and cationic stress phenotypes associated with loss of Pho4 (Figure 1C). No genes implicated in superoxide tolerance were identified, but a comparison of the Pho4-dependent gene set to the cationic stress–induced regulon in *C. albicans* (Enjalbert *et al.*, 2006) revealed an overlap of five genes: *C3_01540W_A*, *C3_02140C_A*, *C6_03320W_A*, *GPD2* and *RHR2*. Three of these genes are of unknown function, but *GPD2* and *RHR2* work in tandem to produce glycerol, an osmoprotectant and a source of phosphate. Northern blotting confirmed that the induction of *GPD2* and *RHR2* seen in wild-type cells after P$_i$ limitation is impaired in *pho4Δ* cells (Figure 5C). NaCl-induced induction of *GPD2* and *RHR2* depends on the

Hog1 SAPK (Enjalbert *et al.*, 2006). However, Pho4 was entirely dispensable for the cationic stress–induced increase in *GPD2* and *RHR2* mRNA levels (unpublished data), which is consistent with the lack of nuclear accumulation of Pho4 after cationic stress (Figure 3A).

We also examined whether genes with stress-protective functions were deregulated in *pho4Δ* cells under normal, phosphate-replete conditions. Many genes (<1300) were up-regulated twofold or more in *pho4Δ* cells compared with wild-type cells, whereas 49 genes were down-regulated. Thus loss of Pho4 has a significant effect on the *C. albicans* transcriptome even when extracellular levels of phosphate are not limiting. Functional categories that were significantly enriched among the up-regulated genes in *pho4Δ* cells included processes involved in DNA Metabolism, DNA Repair and Response to DNA Damage, Cell Cycle, and Response to Stress (Figure 6). This may reflect the high P$_i$ requirement of DNA replication and that phosphate regulation is linked with cell cycle progression in *S. cerevisiae* (Menoyo *et al.*, 2013). However, the genes up-regulated in *pho4Δ* cells again revealed little overlap (23 genes) with the cationic stress–induced regulon (Enjalbert *et al.*, 2006), with no cellular processes significantly enriched. Thus we found no obvious connection between Pho4-dependent and cationic stress–induced genes in *C. albicans*. Intriguingly, however, three of the four copper-requiring superoxide dismutase genes—*SOD1*, *SOD5*, and *SOD6*—were up-regulated in *pho4Δ* cells under phosphate- replete conditions, whereas the manganese-dependent *SOD3* gene was down-regulated (Supplemental Table S2). The effect of Pho4 loss on *SOD1* and *SOD3* levels was validated by Northern blotting (Figure 5C). Therefore, a key question was, Why was the induction of Cu-*SOD* genes unable to confer superoxide stress resistance to *pho4Δ* cells?

Pho4 is required for Sod1 superoxide dismutase activity

To investigate why *SOD* gene induction failed to trigger superoxide stress resistance in *pho4Δ* cells, we performed in-gel activity assays to assess any effect of Pho4 loss on superoxide dismutase activity. Strikingly, Sod1 activity was lower in *pho4Δ* cells than with the wild-type and *pho4Δ + PHO4* reconstituted strains (Figure 7A). This was even more apparent after exposure of cells to menadione (Figure 7A). A previous phenotypic screen of the transcription factor deletion collection reported that cells lacking *PHO4* are resistant to copper (Homann *et al.*, 2009). In addition, our RNA-Seq experiment revealed that when wild-type (WT) cells up-regulated genes associated with Cu-limiting environments (such as the *CTR1* and *FRE7* genes necessary for Cu acquisition and the Mn-dependent cytosolic *SOD3* enzyme; Li *et al.*, 2015), *pho4Δ* cells did not (Supplemental Table S2, pho4 + P$_i$ vs. WT + P$_i$). Perhaps most significant, however, is the up-regulation of the *CRD2* copper metallothionein gene in *pho4Δ* cells. The sequestration of copper by this metallothionine could possibly account for the apparent copper resistance of *C. albicans pho4Δ* cells. Taken together, these results indicated that copper homeostasis was impaired in some way in *pho4Δ* cells. We confirmed that *pho4Δ* cells are resistant to copper (Figure 7B) and used
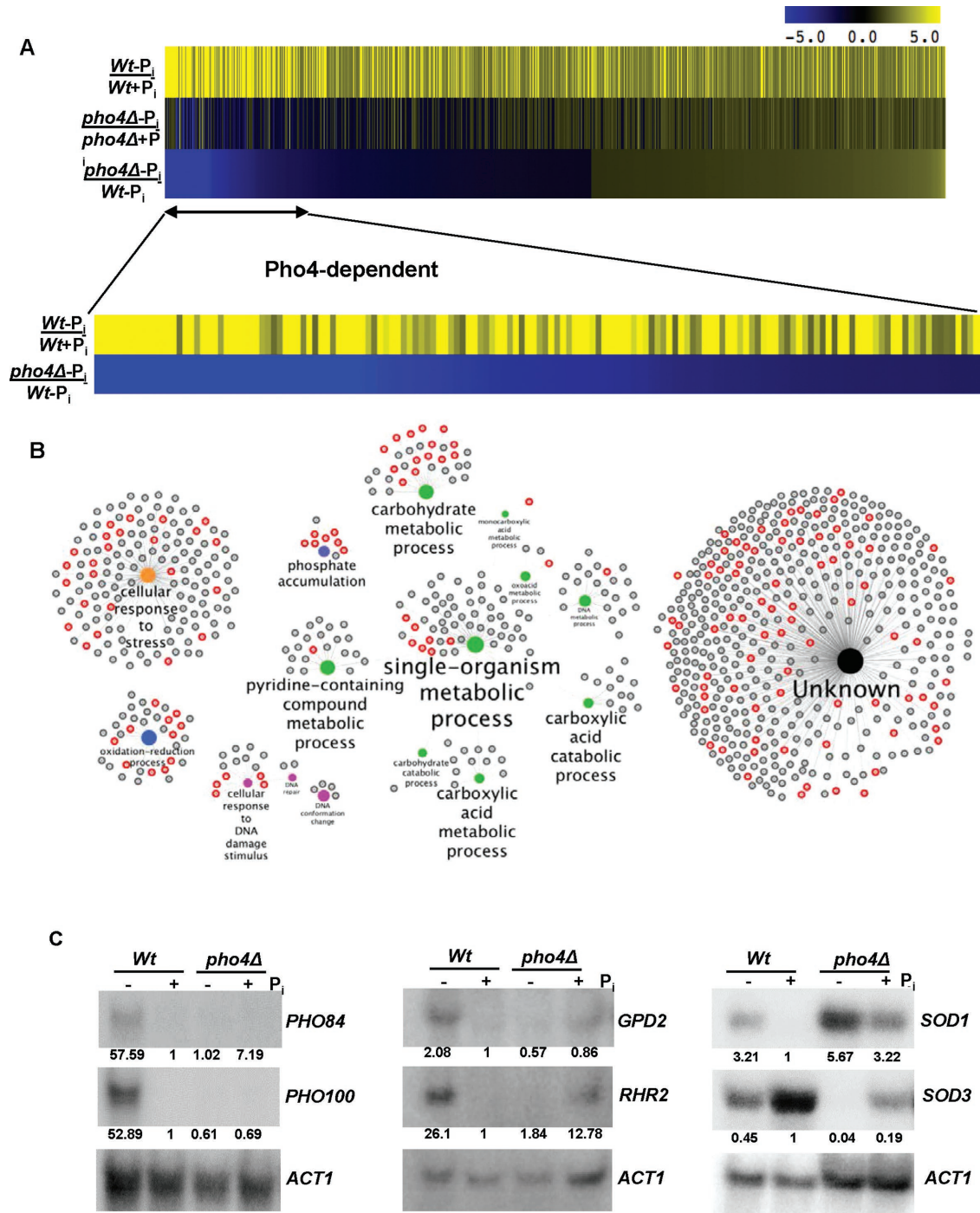
FIGURE 5: Genome response to phosphate limitation in *C. albicans*. (A) Heat map illustrating the fold induction of genes induced (greater than twofold) in wild-type cells after phosphate limitation (top) and fold expression of these genes in *pho4Δ* cells (middle), as measured by RNA-Seq analysis. Of the 822 genes significantly induced in wild-type cells, 150 display a decrease of twofold or lower in *pho4Δ* cells upon comparing the expression ratio *pho4Δ*-P_i/*Wt*-P_i (bottom). These are designated as Pho4-dependent genes. (B) Cytoscape network illustrating all 822 up-regulated genes in wild-type cells after phosphate limitation. Those that display Pho4-dependence are shown in red. GO_Term family members are represented in the same color, and the size of each node representing each GO_Term corresponds to its gene enrichment level. Genes that were mapped according to *Candida* Genome Database Biological Process Unknown are clustered in the category Unknown. (C) Validation of gene expression profiles observed in RNA-Seq analysis. Northern blot analysis of RNA isolated from wild-type (*Wt*) and *pho4Δ* cells following the same −P_i and +P_i conditions used for RNA-Seq experiments. Blots were analyzed with probes specific for the indicated genes, with *ACT1* as a loading control. Fold induction compared with *Wt* cells +P_i.
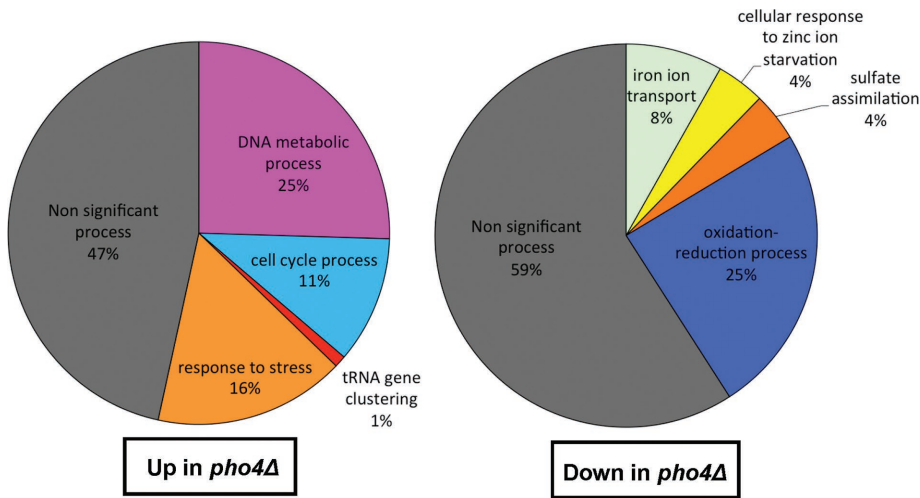
FIGURE 6: Processes deregulated in *pho4Δ* cells under phosphate-replete conditions. Pie charts illustrating the GO biological processes that are deregulated in *pho4Δ* cells compared with wild-type cells when grown in media containing P$_i$. The nonsignificant process category includes all additional processes that were retrieved from GO_Term analysis but did not pass the *p*-value criterion as well as the term Biological Process Unknown.

inductively coupled plasma mass spectrometry (ICP-MS) to determine the effect of Pho4 loss on cellular copper levels in *C. albicans*. However, ICP-MS analysis revealed no change in total cellular copper levels in *pho4Δ* cells compared with wild-type cells (Figure 7C). Thus, although cells lacking Pho4 have wild-type levels of copper, they are resistant to this metal and do not appear to respond as effectively as wild-type cells to a copper-limiting environment. This indicated that Pho4 might play a role in regulating the bioavailability of copper. Indeed, up-regulation of the *CRD2* copper metallothionein could account for the apparent reduction in biological availability of copper in *C. albicans pho4Δ* cells. Defects in the delivery of copper to SODs, such as mutations that inactivate the Ccs1 copper metallochaperone, can be suppressed by addition of excess copper to the growth medium (Rae *et al.*, 1999). Hence we tested whether
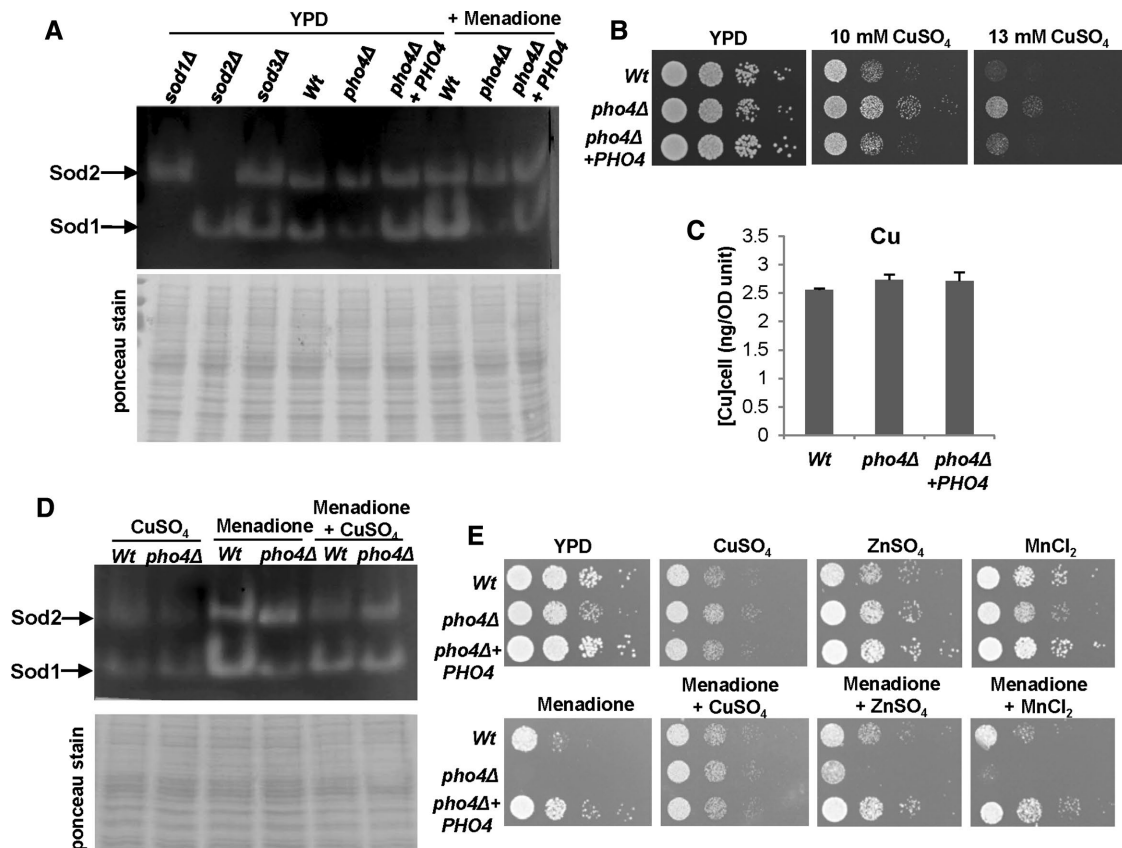

FIGURE 7: Pho4 is required for the activity of the Sod1 superoxide dismutase. (A) Sod1 activity is reduced in cells lacking *pho4Δ*. Extracts were subjected to native PAGE, followed by nitro blue tetrazolium staining to detect superoxide dismutase activity. Duplicate samples were subjected to SDS–PAGE, and after transfer, membranes were stained with Ponceau-S to assess loading. (B) Cells lacking *PHO4* are resistant to copper. Exponentially growing cells were spotted in serial dilutions onto YPD plates containing CuSO$_2$ and incubated for 24 h at 30°C. (C) Effect of *PHO4* loss on intracellular copper levels. Whole-cell nitric acid digests of *Wt*, *pho4Δ*, and *pho4Δ+PHO4* cells grown in YPD were analyzed by ICP-MS. Copper levels are shown as mean ± SD from three independent cultures. (D) Supplementation of media with copper restores Sod1 activity in *pho4Δ* cells. Superoxide dismutase activity was measured as in A. (E) Supplementation of medium with copper rescues the menadione sensitivity of *pho4Δ* cells. Exponentially growing cells were spotted onto YPD plates with or without 300 µM menadione and containing 5 mM CuSO$_2$, 1 mM ZnSO$_4$, or 5 mM MnCl$_2$.
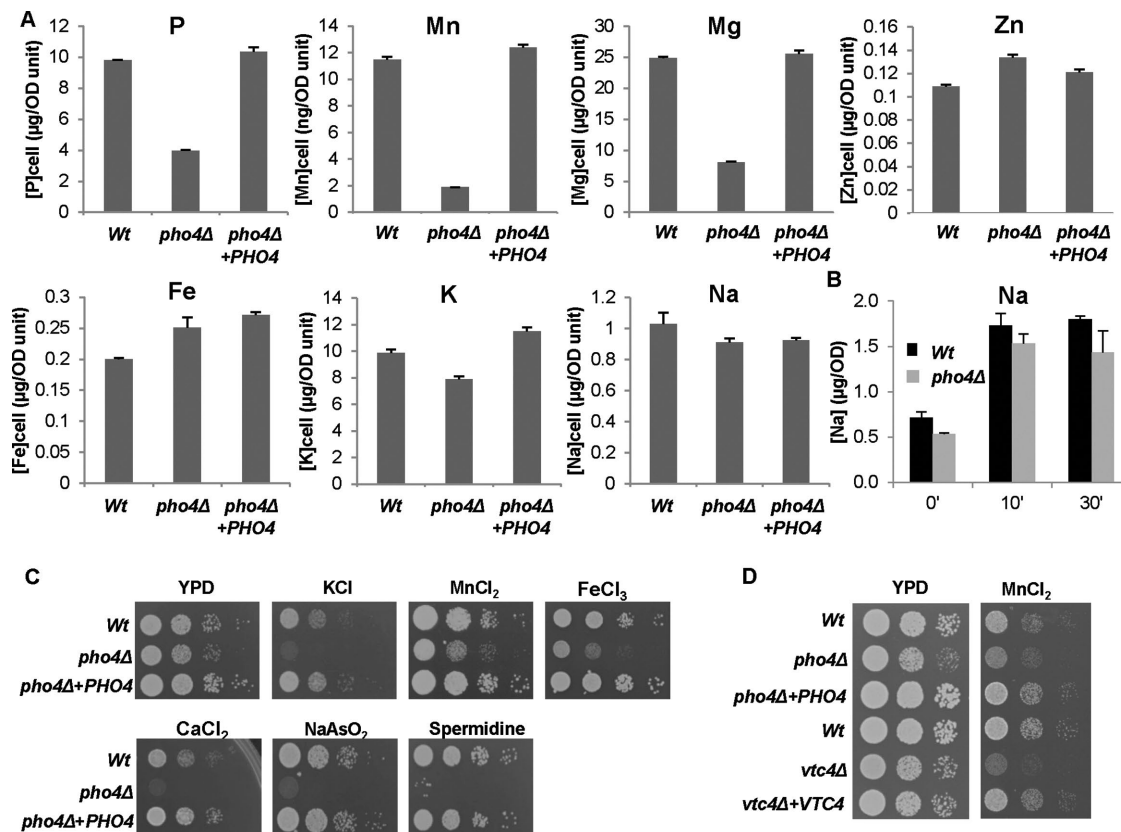
FIGURE 8: Pho4 function is required for metal cation homeostasis and resistance. (A) Effect of *PHO4* loss on intracellular metal levels. Whole-cell nitric acid digests of *Wt*, *pho4Δ*, and *pho4Δ+PHO4* exponentially growing cells in YPD were analyzed by ICP-MS. The results are shown as mean ± SD from three independent cultures. (B) Whole-cell nitric acid digests of *Wt*, *pho4Δ*, and *pho4Δ + PHO4* exponentially grown cells in YPD + 0.5 M NaCl for the indicated times were analyzed by ICP-MS. The results are shown as mean ± SD from three independent cultures. (C) Cells lacking *PHO4* are sensitive to metal and organic cations. Exponentially growing strains were spotted in serial dilutions onto YPD plates containing 0.6 M KCl, 10 mM $MnCl_2$, 5 mM $FeCl_2$, 450 mM $CaCl_2$, 2 mM $NaAsO_2$, or 0.32 μg/ml spermidine. (D) Polyphosphate is important for manganese resistance. Exponentially growing strains were spotted in serial dilutions onto YPD plates containing 5 mM $MnCl_2$. Plates were incubated for 24 h at 30°C.

the Pho4-dependent defects in Sod1 activity and menadione resistance could be rescued by supplementing the growth medium with copper. Strikingly, Sod1 activity was restored to wild-type levels in *pho4Δ* cells in the presence of copper (Figure 7D), and the menadione sensitivity of *pho4Δ* cells was completely rescued (Figure 7E). This rescue was specific to copper, as supplementation of the medium with zinc only marginally rescued the superoxide-sensitive phenotype of *pho4Δ* cells, and manganese addition had no effect (Figure 7E). Taken together, these results indicate that the exquisite sensitivity of *pho4Δ* cells to superoxide is due, at least in part, to a role of Pho4 in mediating copper bioavailability, an essential metal cofactor for the copper/zinc Sod1 enzyme.

Role of Pho4 in metal cation homeostasis
The foregoing findings illustrated that Pho4 function is important in mediating the bioavailability of the metal copper. Of interest, our RNA-Seq data revealed that processes involved in the acquisition of a number of metals in addition to copper were also down-regulated in *pho4Δ* cells (Figure 6). For example, genes involved in iron (*FTR2*, *FET3*), zinc (*ZRT2*, *CSR1*), and copper (*CTR1*, *FRE7*) acquisition were all down-regulated in cells lacking Pho4 compared with wild-type cells (Supplemental Table S2, pho4 + P_i vs. WT + P_i). This suggested perhaps a broader role for Pho4 in regulating metal homeostasis. To

investigate this, we used ICP-MS analysis to determine whether loss of *PHO4* affected the cellular levels of a range of metal cations. As illustrated in Figure 8A, *C. albicans pho4Δ* cells containing lower cellular phosphorous levels (~40% of wild type) also contained notably lower levels of manganese (~16%) and magnesium (~30%) compared with wild-type cells ($p < 0.01$). Possibly related to this, cells lacking *PHO4* displayed impaired growth on medium containing manganese (Figure 8C). Because cells lacking *PHO4* are deficient in the phosphate storage molecule polyP, which is predicted to be able to chelate metal cations due to its high negative charge, we examined whether polyP synthesis was also important for manganese resistance in *C. albicans*. Indeed, polyP-deficient *vtc1Δ* and *vtc4Δ* cells displayed similar enhanced sensitivity to manganese as the *pho4Δ* mutant (Figure 8D and Supplemental Figure S2A). Thus the potential role of polyP in sequestering excess manganese in *C. albicans* likely underlies the impaired resistance of *pho4Δ* cells to this metal.

In contrast to manganese and magnesium, an analysis of the cellular levels of other metal cations in *pho4Δ* cells revealed more modest differences. Levels of zinc and iron were higher in *pho4Δ* cells (123 and 125%, respectively) than in wild-type cells, whereas levels of sodium and potassium were lower (89 and 80%, respectively; Figure 8A). All such differences, with the exception of sodium, were
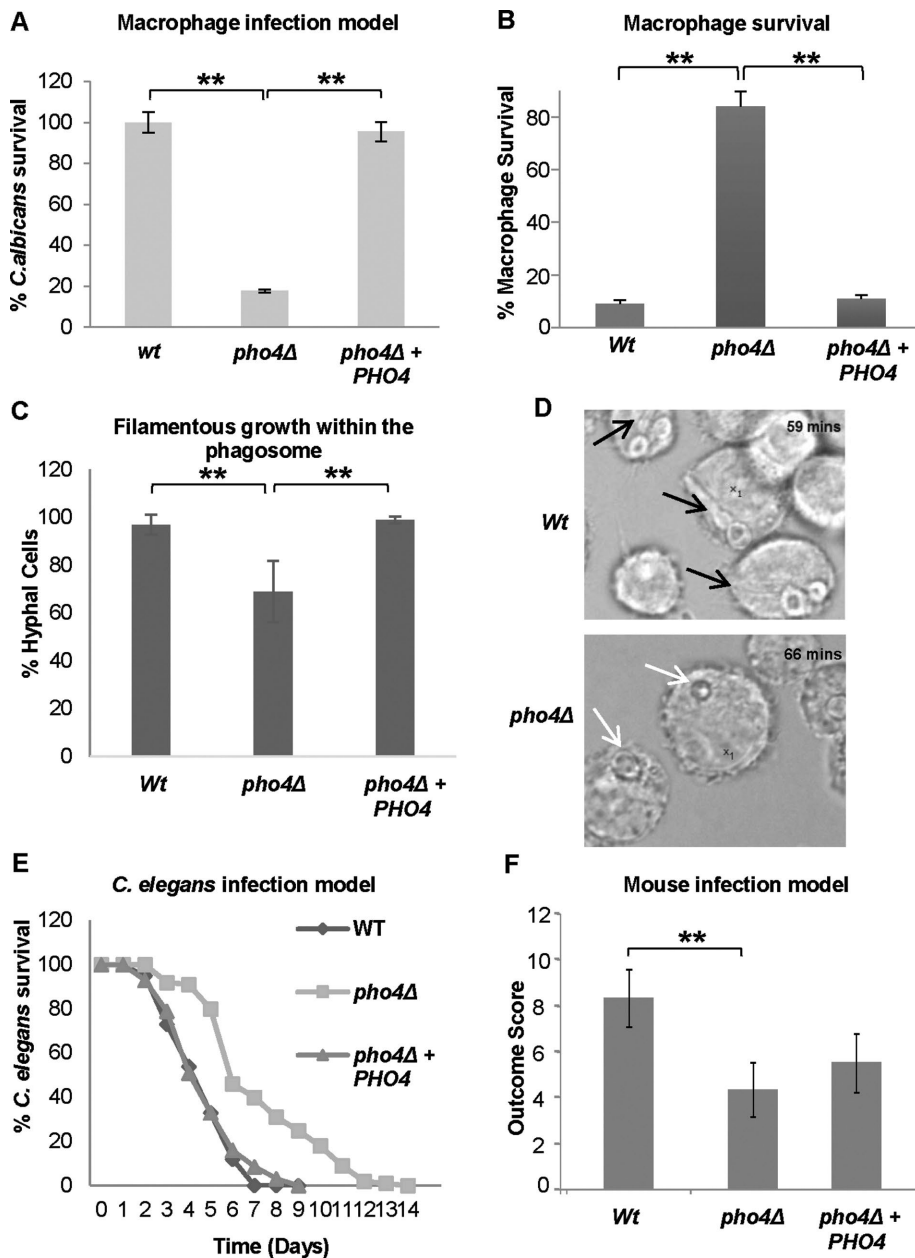
FIGURE 9: Pho4 is required for *C. albicans* virulence in macrophage and animal infection models. (A) Macrophage model of infection. Percentage of *C. albicans* killed after coincubation with J774.1 macrophages (**$p < 0.01$). (B) Macrophage survival. Percentage of macrophages killed after coculture with the indicated *C. albicans* strains (**$p \leq 0.01$). (C) Percentage of *C. albicans* cells that undergo filamentation after phagocytosis. (**$p \leq 0.01$). (D) Cells lacking *PHO4* display defective intracellular hyphal formation after phagocytosis. Images were taken from videos; numbers indicate time of the phagocytic events. Black arrows indicate positioning of *C. albicans* hyphal cells within the macrophage; white arrows indicate nonfilamentous cells. (E) *C. elegans* model of infection. *C. albicans* cells lacking *PHO4* displayed significantly impaired killing of the nematodes compared with *Wt* and *pho4Δ+PHO4* reconstituted strains ($p < 0.001$). Nematodes ($n = 65, 68, 69$) were infected with *Wt*, *pho4Δ*, and *pho4Δ+PHO4* strains, respectively, and survival monitored daily. These data are from a single experiment representative of three independent biological replicates. (F) Mouse model of infection. Outcome score measurements of mice ($n = 6$) infected with the indicated strains. Comparison of *Wt*- and *pho4Δ*-infected groups by Kruskal–Wallis statistical analysis demonstrated a significant difference with *pho4Δ*-infected mice giving a significantly lower outcome score (**$p \leq 0.01$).

significant ($p < 0.01$). We asked whether the NaCl toxicity exhibited by *pho4Δ* cells (Figure 1C) was due to the excess accumulation of sodium after NaCl stress. However, similar increases in sodium levels

were observed in *pho4Δ* and wild-type cells after exposure to NaCl (Figure 8B). Nonetheless, despite modest differences in the intracellular levels of a number of metal cations, cells lacking *PHO4* were significantly more sensitive than wild-type cells to a range of different metals, including sodium (Figure 1C), potassium, calcium, and iron (Figure 8C). In contrast to manganese, polyP function was not required for resistance to any of these other metals (Supplemental Figure S2A). Because the impaired growth exhibited by *pho4Δ* cells in the presence of metal cations does not always correlate with drastic effects on intracellular levels of the metals, we reasoned that maintaining the levels of the abundant phosphate anion within the cell might underlie the role of Pho4 in cation resistance. Consistent with this hypothesis, loss of *PHO4* also affects the cellular resistance to the organic cation spermidine, in addition to the broad range of biologically important metal cations (Figure 8C).

Pho4 is required for virulence in multiple infection models

Given that cells lacking Pho4 are particularly sensitive to stresses encountered after phagocytosis, such as superoxide anions and cationic fluxes (Figure 1), we explored the effect of *PHO4* loss upon *C. albicans*-macrophage interactions. *pho4Δ* cells were acutely sensitive to macrophage-mediated killing compared with the wild type and reconstituted controls ($p < 0.01$; Figure 9A). To explore this further, we infected macrophages with wild-type, *pho4Δ*, and *pho4Δ + PHO4* cells and followed the phagocytic process by live-cell videomicroscopy. Quantitatively, there were no significant differences between the migration speed of J774.1 macrophages toward wild-type or *pho4Δ* mutant cells or in rate of engulfment of fungal cells (unpublished data). However, cells lacking the Pho4 transcription factor were significantly defective in killing macrophages (Figure 9B) and displayed impaired filamentation after phagocytosis (Figure 9, C and D).

After this, we examined the effect of Pho4 loss on *C. albicans* virulence in animal models of infection. First, we used the invertebrate model host *Caenorhabditis elegans* (Pukkila-Worley et al., 2009). The survival of *C. elegans* was significantly extended after infection with *pho4Δ* cells compared with wild-type and *pho4Δ + PHO4* cells ($p < 0.001$), clearly illustrating the importance of Pho4 in mediating *C. albicans* virulence in this infection model (Figure 9E). Next we used the 3-d murine intravenous challenge model of *C. albicans* infection (MacCallum et al., 2009b, 2010). This

model eliminates the need for standard 28-d survival experiments and combines weight loss and kidney fungal burden measurements after 3 d of infection to give an outcome score calculated as log(renal colony-forming units [CFU]/gram) − (0.5 × percentage weight change), with a higher score indicating greater virulence. Previous studies showed a strong correlation between mouse body weight loss over 3 d and kidney fungal burdens at 3 d after intravenous challenge with *C. albicans* and survival times up to 28 d (MacCallum *et al.*, 2009a, 2010). Thus this model, which has been validated and widely used (Cheetham *et al.*, 2011; Ene *et al.*, 2012), is used over the standard 28 model to maximize concordance with the 3Rs (replacement, reduction, and refinement). Mice infected with *pho4Δ* cells had a significantly lower outcome score than those with wild-type cells (*p* < 0.01; Figure 9F). This virulence defect was only partially restored in mice infected with the *pho4Δ* + *PHO4* reconstituted strain, possibly due to haploinsufficiency. Indeed, reintroduction of a single copy of *PHO4* only partially rescues the acid phosphatase defect of *pho4Δ* cells (Figure 2B). It is also of interest that although *C. albicans* cells lacking *PHO4* had a significant effect on weight loss, kidney fungal burdens were comparable to those with wild-type cells (Supplemental Figure S3). Similar findings were reported in *Cryptococcus neoformans*, in which cells defective in phosphate acquisition displayed attenuated virulence in a murine model of cryptococcosis, and yet the fungal burdens in the lungs and brain of infected animals were comparable to those of wild-type cells (Kretschmer *et al.*, 2014). Nonetheless, the results from two distinct animal models indicate that in *C. albicans*, the Pho4 transcription factor is important for virulence. Moreover, the attenuated pathogenicity of *pho4Δ* cells observed in the murine infection model is consistent with the importance of Pho4 in preventing macrophage-mediated killing of *C. albicans*.

DISCUSSION

In this study we show that the Pho4 transcription factor plays vital roles in stress resistance and virulence in *C. albicans*. Because Pho4 does not appear to directly regulate stress-protective genes, we propose that the stress sensitivities exhibited by the *pho4Δ* mutant may be linked to the reduced intracellular phosphate levels in this mutant. This adds to an emerging concept that metabolism and stress resistance are intricately linked in this major pathogen of humans (Brown *et al.*, 2014a). A model summarizing the multifaceted roles of Pho4 in mediating *C. albicans* stress responses and virulence is shown in Figure 10.

Although there is considerable sequence divergence between the Pho4 transcription factors in *C. albicans* and *S. cerevisiae*, we show that *C. albicans* Pho4 accumulates in the nucleus in P_i-limiting environments and regulates both phosphate acquisition and polyP synthesis. A comparison of the Pho4-regulated genes in *C. albicans* with those identified in *S. cerevisiae* (Zhou and O'Shea, 2011) identified a core set of 10 genes. These include the *PHO81* CDK inhibitor, phosphate transporters (*PHO84*), acid phosphatases (*PHO112*, *PHO113*), polyphosphate synthase components (*VTC1*, *VTC3*), enzymes required for phosphate acquisition from glycerophosphodiesters (*GIT1*, *GDE3*) or glycerol-3-phosphate (*RHR2*), and a transporter of ferrichrome siderophores (*SIT1/ARN4*). Consistent with reports in *S. cerevisiae* that a phosphate starvation response is triggered upon growth in alkaline environments (Serrano *et al.*, 2002), exposure of *C. albicans* to alkaline pH stress also results in rapid mobilization of polyP and nuclear accumulation of Pho4. Taken together, these results strongly suggest that the critical role of the *C. albicans* Pho4 transcription factor after exposure to phosphate-limiting or alkaline environments is to induce a gene expression
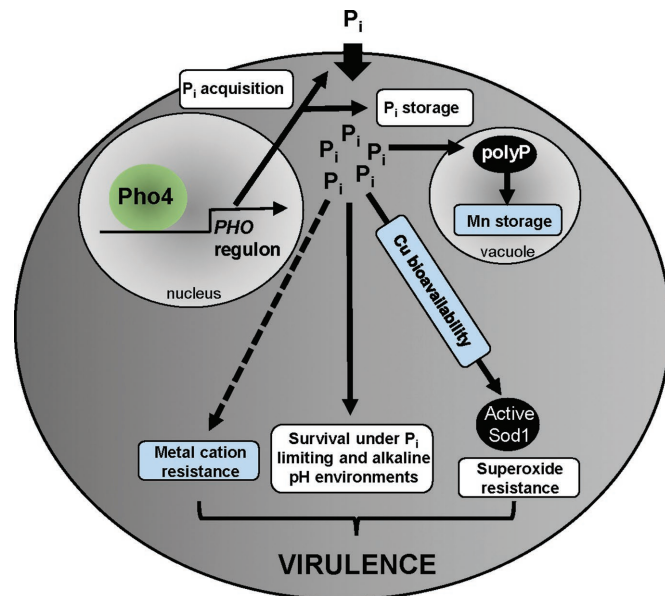

FIGURE 10: Model integrating Pho4 function with stress resistance and virulence phenotypes. The processes linking Pho4 function with metal homeostasis are shown in blue.

program that promotes phosphate acquisition and storage as polyP. It is also likely that the slightly slow-growth phenotype of *pho4Δ* cells is due to reduced intracellular phosphate levels, which may delay cell cycle progression. In *S. cerevisiae*, genes within the *PHO* regulon are specifically induced during M phase to meet the high metabolic demands of P_i associated with mitosis (Neef and Kladde, 2003).

PolyP function has been extensively studied in bacteria, in which it is linked to multiple processes, including growth, stress responses, biofilm formation, and virulence (reviewed in Rao *et al.*, 2009). These diverse phenotypes may be linked to recent findings that polyP functions as a protein chaperone in bacteria (Gray *et al.*, 2014). Less is known, however, about polyP function in eukaryotic cells, although in lower eukaryotes, polyP has been linked to stress adaptation and osmoregulation (reviewed in Docampo *et al.*, 2010). For example, exposure of *Trypanosoma cruzi* to hypo-osmotic stress results in rapid mobilization of polyP, whereas hyper-osmotic stress triggers an increase in polyP level (Ruiz *et al.*, 2001). In this study, we report the first phenotypic characterization of *C. albicans* mutants that lack polyP. Whereas polyP is mobilized in *C. albicans* after hypo-osmotic stress (Supplemental Figure S2C), hyper-osmotic stress, and growth in alkaline pH conditions (Figure 3, C and D), polyP is dispensable in mediating resistance to such stresses (Supplemental Figure S2A). However, polyP is required for manganese resistance, and our data suggest that polyP plays an important role in the sequestration of this metal in *C. albicans* (Figure 8D and Supplemental Figure S2A).

Although cells lacking Pho4 are acutely sensitive to both cationic and superoxide stress, this appears to be independent of this transcription factor regulating the induction of stress-protective genes. Instead, we propose that many of the stress phenotypes exhibited by *pho4Δ* cells relate to the effect of intracellular phosphate on metal homeostasis. Because negatively charged inorganic compounds such as phosphate can bind metal cations, it is beginning to emerge that metal–phosphate interactions play important mechanistic roles in regulating cellular metal homeostasis (Rosenfeld *et al.*, 2010). *S. cerevisiae* cells lacking the negative regulator of Pho4, the Pho80

cyclin, display constitutively high levels of cytosolic phosphate, and this has widespread effects on metal cation accumulation and toxicity (Rosenfeld *et al.*, 2010). Dramatic increases in cellular levels of calcium and sodium occur in *pho80Δ* cells, together with an increased toxicity toward these and other metal cations (Rosenfeld *et al.*, 2010). In addition, a phosphate transporter mutant (*pho84Δ/pho840Δ/pho 89Δ*) in the pathogenic fungus *C. neoformans* was shown to exhibit low phosphate but high intracellular levels of sodium, iron, and zinc (Kretschmer *et al.*, 2014). In this study, we present several lines of evidence to connect phosphate accumulation with metal cation homeostasis and resistance in *C. albicans.* We show that *pho4Δ* cells, which have reduced cellular levels of phosphate, display impaired resistance to a broad number of metal cations (Figure 8C). Such cells also exhibit substantial to moderate differences in the cellular levels of a range of metal cations (Figure 8A) and impaired metal acquisition responses under conditions in which such responses are stimulated in wild-type cells (Figure 6). Although we have not formally proven that defects in intracellular phosphate levels underlie the metal cation homeostasis and resistance phenotypes of *pho4Δ* cells, many of our observations indicate an important role of the phosphate anion in maintaining a charge balance in the cell. This is supported by our observations that Pho4 is vital for resistance to both metal and nonmetal cations in *C. albicans* (Figure 8).

A notable exception to the metal cation–sensitive phenotypes exhibited by *pho4Δ* cells is the significant resistance displayed to copper (Figure 7). Yeast cells tightly regulate copper uptake and storage due to the ability of copper to participate in redox reactions and compete with zinc or iron–sulfur clusters for cysteine-rich metal-binding sites. In *C. albicans*, as in *S. cerevisiae*, copper-limiting conditions trigger activation of the Mac1 transcription factor, which drives the expression of copper acquisition genes such as *CTR1* and *FRE7* (Marvin *et al.*, 2004). Resistance to excess copper is provided by the Crp1 P1-type ATPase copper transporter and the copper metallothioneins Cup1 and Crd2 (Riggle and Kumamoto, 2000; Weissman *et al.*, 2000). The expression of *CRP1* and *CUP1* is induced in high-copper environments, whereas *CRD2* expression seems to be insensitive to copper levels (Riggle and Kumamoto, 2000; Weissman *et al.*, 2000). Because intracellular copper levels are maintained at extremely low levels, copper chaperones are necessary to deliver copper to target enzymes, and, in *C. albicans*, the Ccs1 copper chaperone transfers copper to the copper-containing Sod1 enzyme (Gleason *et al.*, 2014). We examined the RNA-Seq data generated in this study to determine whether any of the genes involved in copper homeostasis are deregulated in *pho4Δ* cells. The *CTR1* and *FRE7* genes, necessary for high-affinity copper transport, are not induced in the *pho4Δ* mutant when up-regulation is observed in wild-type cells (Supplemental Table S2; *pho4Δ* + P_i vs. WT + P_i). Perhaps most significant, however, is the up-regulation of the *CRD2* copper metallothionein gene (4.7-fold) in *pho4Δ* cells. The sequestration of copper by this metallothionine could possibly account for the apparent reduction in biological availability of copper in *C. albicans pho4Δ* cells. It is noteworthy that a connection between intracellular copper and phosphate levels has been implicated in *S. cerevisiae*, in that a number of genes in the *PHO* regulon were up-regulated in cells expressing a constitutively active Mac1 mutant (Gross *et al.*, 2000). Because up-regulation of such genes depended on Pho4, and not Mac1, this suggests that the constitutive activation of Mac1 leads to depletion of the intracellular phosphate pool in *S. cerevisiae*. It is not clear why expression of a constitutively active Mac1 mutant triggers a reduction in intracellular phosphate levels (Gross *et al.*, 2000). Assuming that this is a physiological response to increased intracellular copper levels, cells that are constitutively deficient in intracellular phosphate (such as *pho4Δ* cells) may evoke compensatory mechanisms to deal with copper toxicity such as up-regulation of copper metallothionines, which in turn affects the bioavailability of and toxicity to this metal.

The importance of investigating the relationship between intracellular phosphate levels and copper bioavailability is highlighted by our findings, which indicate that the superoxide-sensitive phenotype of *pho4Δ* cells is due to defects in copper homeostasis and bioavailability. *C. albicans* has developed sophisticated mechanisms to counteract high levels of superoxide stress, including the unusual expansion of the *SOD* superoxide dismutase gene family (Broxton and Culotta, 2016) to include, among other enzymes, two cytoplasmic Sods—Cu/Zn-Sod1 and Mn-Sod3 (Lamarre *et al.*, 2001; Hwang *et al.*, 2002). The rationale for two distinct cytoplasmic enzymes was recently revealed, in that copper availability within the host dictates whether *C. albicans* expresses Cu-dependent *SOD1* or Cu-independent *SOD3* (Li *et al.*, 2015). Thus, even in copper-limiting environments, *C. albicans* is well equipped via the action of Mn-Sod3 to counteract superoxide stress. However, Sod1 activity is impaired in *pho4Δ* cells due to apparent defects in copper availability, as both superoxide stress resistance and Sod1 activity can be restored to wild-type levels upon supplementation of the growth medium with excess copper (Figure 7). Moreover, our RNA-Seq data showed that *pho4Δ* cells failed to switch to Mn-*SOD3* expression under conditions that triggered this switch in wild-type cells (Figure 5C), indicating impaired or delayed ability of the Pho4 mutant to sense copper-limiting environments. Future experiments are aimed at examining the cellular distribution of copper in *pho4Δ* cells compared with wild-type cells, as this will help to define the mechanism(s) linking intracellular phosphate levels with copper sensing and bioavailability. In this regard, it is noteworthy that defects in phosphate homeostasis have been found to affect metal bioavailability in *S. cerevisiae* (Rosenfeld *et al.*, 2010). Specifically, a robust iron starvation response was elicited in *S. cerevisiae* cells with an increased cytoplasmic phosphate content despite wild-type levels of intracellular iron (Rosenfeld *et al.*, 2010).

Our observations that Pho4 is important for *C. albicans* virulence in animal infection models is consistent with studies demonstrating that the Pho4-regulated phosphate transporter gene *PHO84* is up-regulated in multiple host environments (Thewes *et al.*, 2007; Walker *et al.*, 2009) and that the Pho4 target genes *GIT3* and *PHO100* are required for full virulence in murine models of candidiasis (MacCallum *et al.*, 2009b; Bishop *et al.*, 2013). We also find that cells lacking Pho4 are exquisitely sensitive to killing by macrophages. Because the *PHO* regulon is not significantly induced after phagocytosis (Fradin *et al.*, 2005), we propose that Pho4 promotes *C. albicans* survival by providing resistance to the cationic and superoxide stresses encountered after macrophage uptake. This is supported by observations that Sod1, which requires Pho4 function for activity, is important for *C. albicans* survival after phagocytosis (Hwang *et al.*, 2002), as are key regulators of *C. albicans* cationic stress resistance (Arana *et al.*, 2007). Whether defects in phosphate acquisition impair cationic stress resistance and Sod activity in other fungi is worth investigating, as these are important virulence determinants in a range of pathogenic species (Narasipura *et al.*, 2003; Jiang *et al.*, 2011; Jung *et al.*, 2012; Xie *et al.*, 2012). Indeed, a recent study indicates this may be the case, as a *C. neoformans* phosphate transporter mutant displayed metal homeostasis defects and impaired survival in macrophages (Kretschmer *et al.*, 2014).

In conclusion, we show that the Pho4 transcription factor plays multifaceted roles in promoting stress resistance and virulence in

Strain	Name	Genotype	Source
SN148		*arg4Δ/arg4Δ leu2Δ/leu2Δ his1Δ/his1Δ ura3Δ::imm^434/ura3Δ::imm^434 iro1Δ::imm^434/iro1Δ::imm^434*	Noble and Johnson (2005)
SN152		*arg4Δ/arg4Δ leu2Δ/leu2Δ his1Δ/his1Δ URA3/ura3Δ::imm^434 IRO1/ iro1Δ::imm^434*	Noble and Johnson (2005)
ΔΔorf19.2961		*SN152 arg4Δ/arg4Δ leu2Δ/leu2Δ his1Δ/his1Δ URA3/ura3Δ::imm^434 IRO1/iro1Δ::imm^434 pho4Δ::HIS1/pho4Δ::LEU2*	Homann *et al.* (2009)
JC1936	*Wt*	*SN152 arg4Δ/arg4Δ leu2Δ/leu2Δ his1Δ/his1Δ ura3/ura3Δ::imm^434 IRO1/iro1Δ::imm^434 Clp10*	This study
JC1928	*pho4Δ*	*SN152 arg4Δ/arg4Δ leu2Δ/leu2Δ his1Δ/his1Δ ura3/ura3Δ::imm^434 IRO1/iro1Δ::imm^434 pho4Δ::HIS1/pho4Δ::LEU2 Clp10*	This study
JC1917	*pho4Δ + PHO4*	*SN152 arg4Δ/arg4Δ leu2Δ/leu2Δ his1Δ/his1Δ ura3/ura3Δ::imm^434 IRO1/iro1Δ::imm^434 pho4Δ::HIS1/pho4Δ::LEU2 Clp10-PHO4*	This study
JC1977	*PHO4-GFP*	*SN148 pACT-PHO4-GFP:URA3*	This study
JC747	*Wt*	*SN148 Clp30*	da Silva Dantas *et al.* (2010)
JC1983	*vtc1Δ*	*SN148 vtc1Δ::loxP-ARG4-loxP/vtc1Δ::loxP-HIS1-loxP Clp10*	This study
JC1984	*vtc4Δ*	*SN148 vtc4Δ::loxP-ARG4-loxP/vtc4Δ::loxP-HIS1-loxP Clp10*	This study
JC2087	*vtc4Δ + VTC4*	*SN148 vtc4Δ::loxP-ARG4-loxP/vtc4Δ::loxP-HIS1-loxP Clp10-VTC4*	This study
JC50	*hog1Δ*	*ura3::λimm434/ura3 :: λimm434 his1::hisG/his1::hisG hog1Δ:: loxP-ura3-loxP, hog1Δ ::loxP-HIS1-loxP Clp20*	Smith *et al.* (2004)
CA-IF003	*sod1Δ*	*SN152 sod1Δ::LEU2/sod1Δ::HIS1*	Frohner *et al.* (2009)
CA-IF007	*sod2Δ*	*SN152 sod2Δ::LEU2/sod2Δ::HIS1*	Frohner *et al.* (2009)
CA-IF0011	*sod3Δ*	*SN152 sod3Δ::LEU2/sod3Δ::HIS1*	Frohner *et al.* (2009)

TABLE 2: Strains used in this study.

the major fungal pathogen *C. albicans*. Because many of the Pho4-attributed phenotypes relate to metal homeostasis, this study has found a novel layer of homeostatic regulation in *C. albicans*. Furthermore, because metal acquisition and detoxification strategies are vital for fungal survival at the host/pathogen interface (Ding *et al.*, 2014), the role of Pho4 in metal homeostasis merits study in other eukaryotic pathogens.

MATERIALS AND METHODS
Animal studies
All animal experiments were conducted in compliance with United Kingdom Home Office licenses for research on animals (project license number PPL 60/4135) and approved by the University of Aberdeen Ethical Review Committee. Animal experiments were minimized, and all animal experimentation was performed using approaches that minimized animal suffering and maximized our concordance with the 3Rs.

Media
C. albicans strains were routinely grown at 30°C in YPD medium (2% bactopeptone, 1% bacto–yeast extract, 2% glucose; Sherman, 1991). For phosphate-limiting conditions, strains were grown in YPD minus phosphate (YPD $-P_i$) medium in which potassium phosphate was substituted with potassium chloride (2% bactopeptone, 1% yeast extract base without phosphate [ForMedium, Norfolk, UK], 2% glucose) or PNMC $-P_i$ medium (peptone, 2.5 g/l; NaCl, 3 g/l; $MgSO_4$, 1 mM; $CaCl_2$, 1 mM) supplemented with glucose (20%) and ammonium sulfate (5 g/l) as described previously (Romanowski *et al.*, 2012). YPD $-P_i$ and PNMC $-P_i$ media were supplemented with 10 mM KH_2PO_4 phosphate (pH 6) to generate YPD $+ P_i$ and PNMC $+ P_i$, respectively.

Strain construction
The strains used in this study are listed in Table 2, and the oligonucleotides used in their construction are available upon request. The *pho4Δ* strain was derived from a published transcription factor deletion collection (Homann *et al.*, 2009). To reintegrate *PHO4*, the open reading frame (ORF) plus promoter and terminator regions were amplified by PCR using the primer pair PHO4BamH1C1/PHO-4BamH1C2 and ligated into the *Bam*H1 site of Clp10 to generate Clp10-PHO4. Clp10 and Clp10-PHO4 were linearized with *Stu*I and integrated at the *RPS1* locus in a 5-fluoroorotic acid (5-FOA)–resistant derivative of *pho4Δ* to generate auxotropically identical *pho4Δ* (JC1928) and *pho4Δ + PHO4* (JC1917) strains. To generate wild-type cells auxotropically identical to *pho4Δ* null and reconstituted strains, Clp10 was linearized with *Stu*I and integrated into a 5-FOA–resistant derivative of the library wild-type reference strain SN152 to generate JC1936. Hence, in the wild-type (*Wt*; JC1936), *pho4Δ* (JC1928), and *pho4Δ + PHO4* (JC1917) strains, *URA3* is expressed from the *RPS1* locus, which negates the influence of *URA3* expression levels on subsequent virulence assays (Brand *et al.*, 2004).

Deletion of VTC1 and VTC4. To delete *VTC1*, disruption cassettes containing the *HIS1* or *ARG4* gene flanked by *loxP* sites and 91 base pairs 5' and 3' to the *VTC1* ORF were generated by PCR using Vtc1delF and Vtc1delR oligonucleotide primers and the plasmid template pLHL or pLAL (Dennison *et al.*, 2005). Disruption cassettes were sequentially transformed into SN148 wild-type *C. albicans* cells (Noble and Johnson, 2005) to disrupt both alleles of *VTC1*. The same strategy was used to cleanly delete *VTC4*, using the oligonucleotide pair Vtc4delF/Vtc4delR. Disruption of each allele was confirmed by PCR, and Clp10 was integrated at the *RSP1* locus to restore uridine prototrophy (Murad *et al.*, 2000), generating *vtc1Δ* (JC1983) and

vtc4Δ (JC1984) strains. To reintegrate *VTC4* into the respective *vtc4Δ* null strain, the ORF plus promoter and terminator regions was amplified by PCR using primer pair VTC4BamH1C1/VTC4BamH1C2 and ligated into the *Bam*H1 site of Clp10 to generate CIP10-VTC4. Clp10-VTC4 was linearized with *Stu*I and integrated at the *RPS1* locus in *vtc4Δ* cells, generating the *vtc4Δ + VTC4* reconstituted strain (JC2087).

Tagging of Pho4. To tag Pho4 at the C-terminus with green fluorescent protein (GFP), the *PHO4* ORF was amplified by PCR using the primers Pho4ACT1GFPF and GFPACT1 and ligated into the *Sal*I site of pACT1-GFP (Barelle *et al.*, 2004). The resulting pACT1-PHO4GFP plasmid was linearized with *Stu*I and integrated at the *RSP10* locus in wild-type cells to generate JC1977. Correct integration at the *RPS1* locus was confirmed by PCR and DNA sequencing.

Quantitative fitness analysis

The *C. albicans* transcription factor deletion collection (Homann *et al.*, 2009) was screened by QFA (Banks *et al.*, 2012) to identify genes required for cationic and superoxide stress resistance. Liquid-to-solid agar 384-format robotic spot tests were performed as follows. Individual mutants from the deletion library were pinned into 96-well plates containing 200 µl of YPD medium in each well with the BioMatrix BM3-SC robot system (S&P Robotics, Toronto, Canada) using a 96-pin (1-mm-diameter) pin tool and grown overnight without shaking at 30°C. Cultures were then diluted 1/100 in 200 µl of YPD medium, grown without shaking for 8 h at 30°C, and spotted onto YPD agar plates and YPD plates containing 1 M NaCl or 300 µM menadione (Sigma-Aldrich, Dorset, UK). The growth of each strain was monitored by photography over time. Solid agar plates were photographed on a spImager (S&P Robotics) with an integrated camera. Manual settings of the camera were as follows: 0.25 s; aperture, F10; white balance, 3700 K; ISO100; image size, large; image quality, fine; image type, .jpg. Culture density was generated from captured photographs using the Integrated Optical Density measure of cell density provided by the image analysis tool Colonyzer (Lawless *et al.*, 2010). A quantitative measure of fitness was then generated using the product of the maximum doubling rate (MDR; doublings/d), which is the inverse of the doubling time and the maximum doubling potential (MDP; doublings). The SIS was obtained for each strain by calculating the exponential growth rate of the mutant relative to wild type.

Stress sensitivity tests

C. albicans strains were grown at 30°C to exponential phase, and then 10-fold serial dilutions were manually spotted onto YPD plates containing the indicated compounds. Plates were incubated at 30°C for 24 h.

Yeast-to-hypha transition assay

To induce morphogenesis, stationary-phase cells were diluted 1:10 in fresh YPD liquid medium containing 10% fetal calf serum (FCS) and incubated at 37°C for 6 h. Differential interference contrast (DIC) images were captured using a Zeiss Axioscope with a 63× oil immersion objective and AxioVision imaging system.

Localization of Pho4-GFP

C. albicans cells expressing GFP-tagged Pho4 (JC1977) were grown to exponential phase and treated with the stresses indicated or, to induce phosphate limitation, washed three times and resuspended in YPD-P$_i$. Cells were treated with the various stresses for the indicated times and samples taken and processed as described previ-

ously (Enjalbert *et al.*, 2006). 4′,6-Diamidino-2-phenylindole (DAPI) and GFP fluorescence were captured using a Zeiss Axioscope with 63× oil immersion objective and 365-nm and 450- to 490-nm wavelengths for DAPI and GFP.

Secreted acid phosphatase assay

Exponential *C. albicans* cells grown in PNMC (Romanowski *et al.*, 2012) + 2 mM P$_i$ were washed and resuspended in PNMC –P$_i$. Cells were spotted onto PNMC agar plates with or without P$_i$ and allowed to grow for 24 h at 30°C. Secreted acid phosphatase activity was detected on plates by an agar-overlay coloration assay as described previously (To *et al.*, 1973). Agar plates containing *C. albicans* colonies were covered with melted agar solution (1%) containing sodium acetate (50 mM, pH 4), naphthyl phosphate (19 µM; Sigma-Aldrich), and Fast blue salt dye (100 µM; Sigma-Aldrich) and incubated at 30°C for 30-60 min. Dark red coloration of the colony indicated secreted acid phosphatase activity.

Polyphosphate analysis

The presence of intracellular polyP granules was determined by light microscopy by Neisser staining of *C. albicans* cells (Gurr, 1965). Paraformaldehyde-fixed cells (Enjalbert *et al.*, 2006) were mounted onto a slide and stained with freshly prepared solution A (methylene blue, 0.1% [Sigma-Aldrich]; glacial acetic acid, 5%; ethanol, 5%) and solution B (crystal violet, 10% in ethanol) for 10–15 s. Slides were rinsed with water, and solution C (chrysoidin Y, 1% [Sigma-Aldrich]) was added for 45 s and rinsed off, and slides were allowed to dry. DIC images were captured using a Zeiss Axioscope with a 63× oil immersion objective and AxioVision imaging system.

For urea-PAGE and toluidine blue staining, RNA was extracted as described previously (Smith *et al.*, 2004), as this procedure also releases polyP. Total RNA (20 µg) containing polyP was resolved by electrophoresis on 15% polyacrylamide TBE-urea gels (Bio-Rad, Hercules, CA) in 1× Tris-borate-EDTA (TBE) buffer. Gels were then fixed with methanol and glycerol, stained in toluidine blue (Sigma-Aldrich), and destained as described previously (Smith and Morrissey, 2007).

RNA analysis

RNA-Seq sample preparation. Overnight cultures of *C. albicans* wild-type (JC1936) and *pho4Δ* (JC1928) cells grown in YPD at 30°C were diluted to an OD$_{660}$ of 0.2 in fresh YPD and grown to mid exponential phase (OD$_{660}$ ≈ 0.6). Cells were washed twice in YPD –P$_i$, resuspended in YPD –P$_i$ to an OD$_{660}$ of 0.05, and grown for 16 h at 30°C. Cells were harvested, washed in ice-cold H$_2$O, and snap frozen in liquid nitrogen. Phosphate was added to the phosphate-starved culture at a final concentration of 20 mM KH$_2$PO$_4$ (pH 6) and cells grown for 2 h before harvesting as described. Total RNA was isolated from frozen cell pellets using Qiazol reagent as per manufacturer's instructions (Qiagen, Manchester, United Kingdom) after mechanical shearing with 425- to 600-µm acid-washed glass beads (Sigma-Aldrich, Dorset, United Kingdom) in an IKA-Vibrax-Vxr at 2200 rpm (B Braun Biotech International, Melsungen, Germany) for 2 min at 2000 rpm. The integrity of total RNA preparations was analyzed on an Agilent Bioanalyzer (Agilent Technologies, Santa Clara, CA) by monitoring the RNA integrity number. RNA samples were isolated in biological triplicates and stored at 80°C until sequencing processing.

RNA-Seq alignment and analysis. Samples were processed through the Ion Torrent Proton sequencer at the Centre for Genome-Enabled Biology and Medicine, University of Aberdeen, Genomics Facility.

Raw fastq files were successively processed in the following order through Fastqc (version 10.1), Trimgalore (version 3.1), Samtools (version 1.19), STAR aligner (version 2.4), and Htseq (version 5.4). Genome alignment was conducted against the C_albicans_SC5314_version_A21-s02-m09-r08 chromosomes file provided by the *Candida* Genome Database (www.candidagenome.org/). Gene expression analysis was performed using Partek Genomics Suite software, version 6.6. GO term analysis was performed in parallel through the *Candida* Genome Database GO Term Finder and the Cytoscape, version 3, Clue GO plug-in (Bindea *et al.*, 2009). Network construction was performed with Cytoscape, version 3, freeware, Venn diagrams through Venny (version 2.0.2) online freeware, and heat maps with TM4 MultiExperiment Viewer (version 4.9). Statistical comparison among GO term enrichment percentages was performed with GraphPad Prism (version 6).

Northern blot analysis. RNA extraction was performed as described previously (Smith *et al.*, 2004). Gene-specific probes were amplified by PCR from genomic DNA using oligonucleotide primers specific for the indicated genes. Phosphoimage analysis was conducted using a GE Typhoon FLA9500 (GE Healthcare Life Sciences, Buckinghamshire, UK) and quantification performed using ImageQuant software.

Inductively coupled plasma mass spectrometry

Exponentially growing cells grown in YPD at 30°C were harvested by centrifugation, washed twice with 25 ml of Tris buffer (50 mM Tris, pH 7.5), incubated in the same buffer containing 10 mM EDTA for 5 min at room temperature to remove surface-bound metal, and then washed twice with 25 ml of the same buffer without EDTA. Washed pellets were digested in 1 ml of 65% (wt/vol) HNO_3 (Merck) and incubated for >48 h at room temperature. The triplicate digested samples were centrifuged ($13,000 \times g$, 20 min), and the supernatants were diluted 1:10 with 2% (wt/vol) HNO_3 solution that contained 20 µg/l Ag and Pt as internal standards and analyzed by ICP-MS essentially as previously described (Tottey *et al.*, 2008). Each sample was analyzed for sodium (^{23}Na), magnesium (^{24}Mg), phosphorus (^{31}P), potassium (^{39}K), calcium (^{44}Ca), manganese (^{55}Mn), iron (^{56}Fe), copper (^{65}Cu), and zinc (^{66}Zn), as well as for silver (^{107}Ag) and platinum (^{195}Pt), using a Thermo X-series ICP-MS operating in collision cell mode (3.0 ml/min 8% H_2 in He as collision gas). Each isotope was analyzed in peak-jump mode 100 times with 30-ms dwell time on three channels with 0.02–atomic mass unit separation, each in triplicate. Metal concentrations were calculated by comparison to matrix-matched elemental standards (containing 0–1000 µg/l each element) analyzed within the same analytical run and normalized according to the OD_{600} recorded for each culture. Differences were tested for statistical significance by one-way analysis of variance (ANOVA; $**p \leq 0.01$).

SOD in-gel activity assay

Mid exponential–phase *C. albicans* cells were harvested by centrifugation and snap frozen in liquid nitrogen before protein extraction. Cells were resuspended in lysis buffer containing 10 mM sodium phosphate (pH 7.8), 5 mM EDTA, 5 mM ethylene glycol tetraacetic acid, 50 mM NaCl, 0.45% (vol/vol) NP-40, and 10% (vol/vol) glycerol (Aguirre *et al.*, 2013). Protein lysates were prepared by bead beating with glass beads and clarification by centrifugation at 13,000 rpm for 10 min at 4°C. Protein extract (50 µg) was subjected to native-PAGE on 12% gels and SOD activity detected by nitro blue tetrazolium staining (Flohe and Otting, 1984). Cells lacking *SOD1* and *SOD2* were used as controls (Frohner *et al.*, 2009). Duplicate sam-

ples were subjected to SDS–PAGE, followed by Ponceau-S staining of membranes to determine protein loading.

Infection assays

C. elegans pathogenesis assay. The method described for pathogen infection of *C. elegans* (Powell and Ausubel, 2008) was adopted with the following modifications. A 10-µl amount of exponential *C. albicans* cells was spotted onto the center of a 4-cm Petri dish containing 7 ml of British Heart Infusion agar, ampicillin (100 µg/ml), and kanamycin (45 µg/ml) and allowed to dry overnight at room temperature. The next day, synchronized L4-stage adult *glp-4 C. elegans* maintained at 25°C were washed from plates containing their normal food source (*Escherichia coli* OP50), and 60–70 worms were transferred to plates seeded with *C. albicans* cells. The *C. elegans glp-4* nematodes are sterile when propagated at the restrictive temperature of 25°C, which prevents progeny formation. Plates were incubated at 25°C, and worm survival was scored daily. Worms were considered to be dead if they did not move in response to probing with a pick and no pharynx contraction was observed. Differences in *C. elegans* survival were determined by the log-rank test. In all experiments, $p < 0.05$ was considered significant.

Murine intravenous challenge assay. Murine BALB/c female mice (6–8 wk old; Harlan, United Kingdom) were housed in randomly assigned groups of six with food and water provided ad libitum. Mice ($n = 6$) were infected intravenously via a lateral tail vein with 4.2e4 CFU/g *C. albicans* wild-type (*Wt*; JC1936), *pho4Δ* (JC1928), and *pho4Δ + PHO4* (JC1917) strains. Body weights were recorded daily. At 72 h after challenge, the animals were weighed and humanely killed, and kidneys were removed aseptically. Fungal burdens were measured by viable counts for two half-kidneys per animal. Virulence outcome scores were determined by assessing renal fungal burden and percentage weight change at 72 h using outcome score = log(renal CFU/g) – (0.5 × percentage weight change) (MacCallum *et al.*, 2009b, 2010). Differences were tested statistically by Kruskal–Wallis statistical analysis.

C. albicans survival after phagocytosis

J774.1 macrophages were seeded at a density of 2×10^5 cells in six-well plates for 24 h. Overnight culture of *C. albicans* cells was added to the macrophages at a multiplicity of infection (MOI) of 3:1 macrophage/candida or to medium without macrophages. Cells were coincubated for 6 h at 37°C, after which, unphagocytosed *C. albicans* cells were washed off and macrophages lysed with Triton X-100 (1%) to release *C. albicans* cells. Cells were plated onto YPD plates and incubated overnight at 30°C, and percentage survival was calculated as (CFUs +macrophages/CFUs −macrophages) × 100. Mean values and SDs were calculated for all phagocytosis assays. Differences were tested for statistical significance by one-way ANOVA ($**p < 0.01$).

Phagocytosis assays and live-cell video microscopy

These experiments were performed as described previously (Bain *et al.*, 2014). The J774.1 mouse macrophage cell line was maintained at 37°C and 5% CO_2 in DMEM (Lonza, Slough, United Kingdom) supplemented with 10% heat-activated FCS (Biosera, Ringmer, United Kingdom). Cells were seeded at a density of 1.2×10^5 cells/well in an eight-well slide and incubated overnight at 37°C and 5% CO_2. Before coincubation, growth medium in wells was replaced with prewarmed, CO_2-independent medium containing 10% FCS (Invitrogen). Overnight cultures of *C. albicans* strains grown in YPD

were washed in sterile phosphate-buffered saline (pH 7.4) and co-cultured with J774.1 cells at a MOI of 3:1. DIC images of cocultured cells were taken at 1-min intervals over a 6-h time course using an Ultra VIEW VoX spinning-disk microscope (Nikon, Surrey, United Kingdom) and an electron-multiplying charge-coupled device camera. Two independent experiments were carried out, and six movies were analyzed from each experiment per *C. albicans* strain. One hundred macrophages were randomly selected from each movie and phagocytic activity determined. Volocity 5.0 imaging software (ImproVision, PerkinElmer, Coventry, United Kingdom) was used for data acquisition and analysis as described previously (Lewis *et al.*, 2012). The software enabled analysis of macrophage migration and provided details on distance traveled and velocity of individual macrophages, from which the mean track velocity was calculated. The software also enabled the determination of the engulfment time, migration rate, rate of *C. albicans* filamentation, and macrophage survival. Macrophage survival/killing was determined by detecting number of ruptured macrophages within sample populations of 100. Differences were tested for statistical significance by one-way ANOVA with Bonferroni's post hoc comparisons.

REFERENCES
Aguirre JD, Clark HM, McIlvin M, Vazquez C, Palmere SL, Grab DJ, Seshu J, Hart PJ, Saito M, Culotta VC (2013). A manganese-rich environment supports superoxide dismutase activity in a Lyme disease pathogen, Borrelia burgdorferi. J Biol Chem 288, 8468–8478.

Alonso-Monge R, Navarro-Garcia F, Molero G, Diez-Orejas R, Gustin M, Pla J, Sanchez M, Nombela C (1999). Role of the mitogen-activated protein kinase Hog1p in morphogenesis and virulence of *Candida albicans*. J Bacteriol 181, 3058–3068.

Arana DM, Alonso-Monge R, Du C, Calderone R, Pla J (2007). Differential susceptibility of mitogen-activated protein kinase pathway mutants to oxidative-mediated killing by phagocytes in the fungal pathogen *Candida albicans*. Cell Microbiol. 9, 1647–1659.

Bain JM, Louw J, Lewis LE, Okai B, Walls CA, Ballou ER, Walker LA, Reid D, Munro CA, Brown AJ, *et al.* (2014). *Candida albicans* hypha formation and mannan masking of beta-glucan inhibit macrophage phagosome maturation. MBio 5, e01874.

Banks AP, Lawless C, Lydall DA (2012). A quantitative fitness analysis workflow. J Vis Exp 66, 4018.

Barelle CJ, Manson CL, MacCallum DM, Odds FC, Gow NA, Brown AJ (2004). GFP as a quantitative reporter of gene regulation in *Candida albicans*. Yeast 21, 333–340.

Bindea G, Mlecnik B, Hackl H, Charoentong P, Tosolini M, Kirilovsky A, Fridman WH, Pages F, Trajanoski Z, Galon J (2009). ClueGO: a Cytoscape plug-in to decipher functionally grouped gene ontology and pathway annotation networks. Bioinformatics 25, 1091–1093.

Bishop AC, Ganguly S, Solis NV, Cooley BM, Jensen-Seaman MI, Filler SG, Mitchell AP, Patton-Vogt J (2013). Glycerophosphocholine utilization by *Candida albicans*: role of the Git3 transporter in virulence. J Biol Chem 288, 33939–33952.

Bishop AC, Sun T, Johnson ME, Bruno VM, Patton-Vogt J (2011). Robust utilization of phospholipase-generated metabolites, glycerophosphodiesters, by *Candida albicans*: role of the CaGit1 permease. Eukaryot Cell 10, 1618–1627.

Brand A, MacCallum DM, Brown AJ, Gow NA, Odds FC (2004). Ectopic expression of URA3 can influence the virulence phenotypes and proteome of *Candida albicans* but can be overcome by targeted reintegration of URA3 at the RPS10 locus. Eukaryot Cell 3, 900–909.

Brown AJ, Brown GD, Netea MG, Gow NA (2014a). Metabolism impacts upon Candida immunogenicity and pathogenicity at multiple levels. Trends Microbiol 22, 614–622.

Brown AJ, Budge S, Kaloriti D, Tillmann A, Jacobsen MD, Yin Z, Ene IV, Bohovych I, Sandai D, Kastora S, *et al.* (2014b). Stress adaptation in a pathogenic fungus. J Exp Biol 217, 144–155.

Brown GD, Denning DW, Gow NA, Levitz SM, Netea MG, White TC (2012). Hidden killers: human fungal infections. Sci Transl Med 4, 165rv113.

Broxton CN, Culotta VC (2016). SOD enzymes and microbial pathogens: surviving the oxidative storm of infection. PLoS Pathog 12, e1005295.

Chaves GM, Bates S, Maccallum DM, Odds FC (2007). *Candida albicans* GRX2, encoding a putative glutaredoxin, is required for virulence in a murine model. Genet Mol Res 6, 1051–1063.

Cheetham J, MacCallum DM, Doris KS, da Silva Dantas A, Scorfield S, Odds F, Smith DA, Quinn J (2011). MAPKKK-independent regulation of the Hog1 stress-activated protein kinase in *Candida albicans*. J Biol Chem 286, 42002–42016.

da Silva Dantas A, Patterson MJ, Smith DA, Maccallum DM, Erwig LP, Morgan BA, Quinn J (2010). Thioredoxin regulates multiple hydrogen peroxide-induced signaling pathways in *Candida albicans*. Mol Cell Biol 30, 4550–4563.

Davis D, Wilson RB, Mitchell AP (2000). RIM101-dependent and -independent pathways govern pH responses in *Candida albicans*. Mol Cell Biol 20, 971–978.

Dennison PM, Ramsdale M, Manson CL, Brown AJ (2005). Gene disruption in *Candida albicans* using a synthetic, codon-optimised Cre-loxP system. Fungal Genet Biol 42, 737–748.

Ding C, Festa RA, Sun TS, Wang ZY (2014). Iron and copper as virulence modulators in human fungal pathogens. Mol Microbiol 93, 10–23.

Docampo R, Ulrich P, Moreno SN (2010). Evolution of acidocalcisomes and their role in polyphosphate storage and osmoregulation in eukaryotic microbes. Philos Trans R Soc Lond B Biol Sci 365, 775–784.

Ene IV, Adya AK, Wehmeier S, Brand AC, Maccallum DM, Gow NA, Brown AJ (2012). Host carbon sources modulate cell wall architecture, drug resistance and virulence in a fungal pathogen. Cell Microbiol 14, 1319–1335.

Enjalbert B, MacCallum DM, Odds FC, Brown AJ (2007). Niche-specific activation of the oxidative stress response by the pathogenic fungus *Candida albicans*. Infect Immun 75, 2143–2151.

Enjalbert B, Smith DA, Cornell MJ, Alam I, Nicholls S, Brown AJ, Quinn J (2006). Role of the Hog1 stress-activated protein kinase in the global transcriptional response to stress in the fungal pathogen *Candida albicans*. Mol Biol Cell 17, 1018–1032.

Flohe L, Otting F (1984). Superoxide dismutase assays. Methods Enzymol 105, 93–104.

Fradin C, De Groot P, MacCallum D, Schaller M, Klis F, Odds FC, Hube B (2005). Granulocytes govern the transcriptional response, morphology and proliferation of *Candida albicans* in human blood. Mol Microbiol 56, 397–415.

Fradin C, Kretschmar M, Nichterlein T, Gaillardin C, d'Enfert C, Hube B (2003). Stage-specific gene expression of *Candida albicans* in human blood. Mol Microbiol 47, 1523–1543.

Frohner IE, Bourgeois C, Yatsyk K, Majer O, Kuchler K (2009). *Candida albicans* cell surface superoxide dismutases degrade host-derived reactive oxygen species to escape innate immune surveillance. Mol Microbiol 71, 240–252.

Gleason JE, Li CX, Odeh HM, Culotta VC (2014). Species-specific activation of Cu/Zn SOD by its CCS copper chaperone in the pathogenic yeast *Candida albicans*. J Biol Inorg Chem 19, 595–603.

Gray MJ, Wholey WY, Wagner NO, Cremers CM, Mueller-Schickert A, Hock NT, Krieger AG, Smith EM, Bender RA, Bardwell JC, *et al.* (2014). Polyphosphate is a primordial chaperone. Mol Cell 53, 689–699.

Gross C, Kelleher M, Iyer VR, Brown PO, Winge DR (2000). Identification of the copper regulon in *Saccharomyces cerevisiae* by DNA microarrays. J Biol Chem 275, 32310–32316.

Gurr E (1965). The Rational Use of Dyes in Biology, London: Hill.

Homann OR, Dea J, Noble SM, Johnson AD (2009). A phenotypic profile of the *Candida albicans* regulatory network. PLoS Genet 5, e1000783.

Hothorn M, Neumann H, Lenherr ED, Wehner M, Rybin V, Hassa PO, Uttenweiler A, Reinhardt M, Schmidt A, Seiler J, *et al.* (2009). Catalytic core of a membrane-associated eukaryotic polyphosphate polymerase. Science 324, 513–516.

Hromatka BS, Noble SM, Johnson AD (2005). Transcriptional response of *Candida albicans* to nitric oxide and the role of the *YHB1* gene in nitrosative stress and virulence. Mol Biol Cell 16, 4814–4826.

Hwang CS, Rhie GE, Oh JH, Huh WK, Yim HS, Kang SO (2002). Copper- and zinc-containing superoxide dismutase (Cu/ZnSOD) is required for the protection of *Candida albicans* against oxidative stresses and the expression of its full virulence. Microbiology 148, 3705–3713.

Jiang J, Yun Y, Fu J, Shim WB, Ma Z (2011). Involvement of a putative response regulator FgRrg-1 in osmotic stress response, fungicide resistance and virulence in *Fusarium graminearum*. Mol Plant Pathol 12, 425–436.

Jung KW, Strain AK, Nielsen K, Jung KH, Bahn YS (2012). Two cation transporters Ena1 and Nha1 cooperatively modulate ion homeostasis, antifungal drug resistance, virulence of *Cryptococcus neoformans* via the HOG pathway. Fungal Genet Biol 49, 332–345.

Kretschmer M, Reiner E, Hu G, Tam N, Oliveira DL, Caza M, Yeon JH, Kim J, Kastrup CJ, Jung WH, *et al.* (2014). Defects in phosphate acquisition and storage influence virulence of *Cryptococcus neoformans*. Infect Immun 82, 2697–2712.

Kuznets G, Vigonsky E, Weissman Z, Lalli D, Gildor T, Kauffman SJ, Turano P, Becker J, Lewinson O, Kornitzer D (2014). A relay network of extracellular heme-binding proteins drives *C. albicans* iron acquisition from hemoglobin. PLoS Pathog 10, e1004407.

Lamarre C, LeMay JD, Deslauriers N, Bourbonnais Y (2001). *Candida albicans* expresses an unusual cytoplasmic manganese-containing superoxide dismutase (SOD3 gene product) upon the entry and during the stationary phase. J Biol Chem 276, 43784–43791.

Lawless C, Wilkinson DJ, Young A, Addinall SG, Lydall DA (2010). Colonyzer: automated quantification of micro-organism growth characteristics on solid agar. BMC Bioinformatics 11, 287.

Lewis LE, Bain JM, Lowes C, Gillespie C, Rudkin FM, Gow NA, Erwig LP (2012). Stage specific assessment of *Candida albicans* phagocytosis by macrophages identifies cell wall composition and morphogenesis as key determinants. PLoS Pathog 8, e1002578.

Li CX, Gleason JE, Zhang SX, Bruno VM, Cormack BP, Culotta VC (2015). *Candida albicans* adapts to host copper during infection by swapping metal cofactors for superoxide dismutase. Proc Natl Acad Sci USA 112, E5336–E5342.

Lorenz MC, Bender JA, Fink GR (2004). Transcriptional response of *Candida albicans* upon internalization by macrophages. Eukaryot Cell 3, 1076–1087.

MacCallum DM, Castillo L, Brown AJ, Gow NA, Odds FC (2009a). Early-expressed chemokines predict kidney immunopathology in experimental disseminated *Candida albicans* infections. PLoS One 4, e6420.

MacCallum DM, Castillo L, Nather K, Munro CA, Brown AJ, Gow NA, Odds FC (2009b). Property differences among the four major *Candida albicans* strain clades. Eukaryot Cell 8, 373–387.

MacCallum DM, Coste A, Ischer F, Jacobsen MD, Odds FC, Sanglard D (2010). Genetic dissection of azole resistance mechanisms in *Candida albicans* and their validation in a mouse model of disseminated infection. Antimicrob Agents Chemother 54, 1476–1483.

Martchenko M, Alarco AM, Harcus D, Whiteway M (2004). Superoxide dismutases in *Candida albicans*: transcriptional regulation and functional characterization of the hyphal-induced *SOD5* gene. Mol Biol Cell 15, 456–467.

Marvin ME, Mason RP, Cashmore AM (2004). The *CaCTR1* gene is required for high-affinity iron uptake and is transcriptionally controlled by a copper-sensing transactivator encoded by CaMAC1. Microbiology 150, 2197–2208.

Menoyo S, Ricco N, Bru S, Hernandez-Ortega S, Escote X, Aldea M, Clotet J (2013). Phosphate-activated cyclin-dependent kinase stabilizes G1 cyclin to trigger cell cycle entry. Mol Cell Biol 33, 1273–1284.

Moreno SN, Docampo R (2013). Polyphosphate and its diverse functions in host cells and pathogens. PLoS Pathog 9, e1003230.

Morgan J (2005). Global trends in candidemia: review of reports from 1995–2005. Curr Infect Dis Rep 7, 429–439.

Murad AM, Lee PR, Broadbent ID, Barelle CJ, Brown AJ (2000). Clp10, an efficient and convenient integrating vector for *Candida albicans*. Yeast 16, 325–327.

Narasipura SD, Ault JG, Behr MJ, Chaturvedi V, Chaturvedi S (2003). Characterization of Cu,Zn superoxide dismutase (*SOD1*) gene knock-out

mutant of *Cryptococcus neoformans var. gattii*: role in biology and virulence. Mol Microbiol 47, 1681–1694.

Neef DW, Kladde MP (2003). Polyphosphate loss promotes SNF/SWI- and Gcn5-dependent mitotic induction of *PHO5*. Mol Cell Biol 23, 3788–3797.

Noble SM, Johnson AD (2005). Strains and strategies for large-scale gene deletion studies of the diploid human fungal pathogen *Candida albicans*. Eukaryot Cell 4, 298–309.

Odds FC (1988). Candida and Candidosis, London: Bailliere-Tindall.

Ogawa N, DeRisi J, Brown PO (2000). New components of a system for phosphate accumulation and polyphosphate metabolism in *Saccharomyces cerevisiae* revealed by genomic expression analysis. Mol Biol Cell 11, 4309–4321.

O'Neill EM, Kaffman A, Jolly ER, O'Shea EK (1996). Regulation of PHO4 nuclear localization by the PHO80-PHO85 cyclin-CDK complex. Science 271, 209–212.

Powell JR, Ausubel FM (2008). Models of *Caenorhabditis elegans* infection by bacterial and fungal pathogens. Methods Mol Biol 415, 403–427.

Prieto D, Roman E, Correia I, Pla J (2014). The HOG pathway is critical for the colonization of the mouse gastrointestinal tract by *Candida albicans*. PLoS One 9, e87128.

Pukkila-Worley R, Peleg AY, Tampakakis E, Mylonakis E (2009). *Candida albicans* hyphal formation and virulence assessed using a *Caenorhabditis elegans* infection model. Eukaryot Cell 8, 1750–1758.

Rae TD, Schmidt PJ, Pufahl RA, Culotta VC, O'Halloran TV (1999). Undetectable intracellular free copper: the requirement of a copper chaperone for superoxide dismutase. Science 284, 805–808.

Rao NN, Gomez-Garcia MR, Kornberg A (2009). Inorganic polyphosphate: essential for growth and survival. Annu Rev Biochem 78, 605–647.

Reeves EP, Lu H, Jacobs HL, Messina CG, Bolsover S, Gabella G, Potma EO, Warley A, Roes J, Segal AW (2002). Killing activity of neutrophils is mediated through activation of proteases by K+ flux. Nature 416, 291–297.

Riggle PJ, Kumamoto CA (2000). Role of a *Candida albicans* P1-type ATPase in resistance to copper and silver ion toxicity. J Bacteriol 182, 4899–4905.

Romanowski K, Zaborin A, Valuckaite V, Rolfes RJ, Babrowski T, Bethel C, Olivas A, Zaborina O, Alverdy JC (2012). *Candida albicans* isolates from the gut of critically ill patients respond to phosphate limitation by expressing filaments and a lethal phenotype. PLoS One 7, e30119.

Rosenfeld L, Reddi AR, Leung E, Aranda K, Jensen LT, Culotta VC (2010). The effect of phosphate accumulation on metal ion homeostasis in *Saccharomyces cerevisiae*. J Biol Inorg Chem 15, 1051–1062.

Rubin-Bejerano I, Fraser I, Grisafi P, Fink GR (2003). Phagocytosis by neutrophils induces an amino acid deprivation response in *Saccharomyces cerevisiae* and *Candida albicans*. Proc Natl Acad Sci USA 100, 11007–11012.

Ruiz FA, Rodrigues CO, Docampo R (2001). Rapid changes in polyphosphate content within acidocalcisomes in response to cell growth, differentiation, and environmental stress in *Trypanosoma cruzi*. J Biol Chem 276, 26114–26121.

Sambade M, Alba M, Smardon AM, West RW, Kane PM (2005). A genomic screen for yeast vacuolar membrane ATPase mutants. Genetics 170, 1539–1551.

Schneider KR, Smith RL, O'Shea EK (1994). Phosphate-regulated inactivation of the kinase PHO80-PHO85 by the CDK inhibitor PHO81. Science 266, 122–126.

Serrano R, Ruiz A, Bernal D, Chambers JR, Arino J (2002). The transcriptional response to alkaline pH in *Saccharomyces cerevisiae*: evidence for calcium-mediated signalling. Mol Microbiol 46, 1319–1333.

Sherman F (1991). Getting started with yeast. Methods Enzymol 194, 3–21.

Smith DA, Nicholls S, Morgan BA, Brown AJ, Quinn J (2004). A conserved stress-activated protein kinase regulates a core stress response in the human pathogen *Candida albicans*. Mol Biol Cell 15, 4179–4190.

Smith SA, Morrissey JH (2007). Sensitive fluorescence detection of polyphosphate in polyacrylamide gels using 4',6-diamidino-2-phenylindol. Electrophoresis 28, 3461–3465.

Stoldt VR, Sonneborn A, Leuker CE, Ernst JF (1997). Efg1p, an essential regulator of morphogenesis of the human pathogen *Candida albicans*, is a member of a conserved class of bHLH proteins regulating morphogenetic processes in fungi. EMBO J 16, 1982–1991.

Thewes S, Kretschmar M, Park H, Schaller M, Filler SG, Hube B (2007). In vivo and ex vivo comparative transcriptional profiling of invasive and non-invasive *Candida albicans* isolates identifies genes associated with tissue invasion. Mol Microbiol 63, 1606–1628.

To EA, Ueda Y, Kakimoto SI, Oshima Y (1973). Isolation and characterization of acid phosphatase mutants in *Saccharomyces cerevisiae*. J Bacteriol 113, 727–738.

Tottey S, Waldron KJ, Firbank SJ, Reale B, Bessant C, Sato K, Cheek TR, Gray J, Banfield MJ, Dennison C, *et al.* (2008). Protein-folding location can regulate manganese-binding versus copper- or zinc-binding. Nature 455, 1138–1142.

Urrialde V, Prieto D, Pla J, Alonso-Monge R (2015). The Pho4 transcription factor mediates the response to arsenate and arsenite in *Candida albicans*. Front Microbiol 6, 118.

Walker LA, Maccallum DM, Bertram G, Gow NA, Odds FC, Brown AJ (2009). Genome-wide analysis of *Candida albicans* gene expression patterns during infection of the mammalian kidney. Fungal Genet Biol 46, 210–219.

Weissman Z, Berdicevsky I, Cavari BZ, Kornitzer D (2000). The high copper tolerance of *Candida albicans* is mediated by a P-type ATPase. Proc Natl Acad Sci USA 97, 3520–3525.

Wilson D, Thewes S, Zakikhany K, Fradin C, Albrecht A, Almeida R, Brunke S, Grosse K, Martin R, Mayer F, *et al.* (2009). Identifying infection-associated genes of *Candida albicans* in the postgenomic era. FEMS Yeast Res 9, 688–700.

Wisplinghoff H, Bischoff T, Tallent SM, Seifert H, Wenzel RP, Edmond MB (2004). Nosocomial bloodstream infections in US hospitals: analysis of 24,179 cases from a prospective nationwide surveillance study. Clin Infect Dis 39, 309–317.

Wysong DR, Christin L, Sugar AM, Robbins PW, Diamond RD (1998). Cloning and sequencing of a *Candida albicans* catalase gene and effects of disruption of this gene. Infect Immun 66, 1953–1961.

Xie XQ, Li F, Ying SH, Feng MG (2012). Additive contributions of two manganese-cored superoxide dismutases (MnSODs) to antioxidation, UV tolerance and virulence of *Beauveria bassiana*. PLoS One 7, e30298.

Zakikhany K, Naglik JR, Schmidt-Westhausen A, Holland G, Schaller M, Hube B (2007). In vivo transcript profiling of *Candida albicans* identifies a gene essential for interepithelial dissemination. Cell Microbiol 9, 2938–2954.

Zhou X, O'Shea EK (2011). Integrated approaches reveal determinants of genome-wide binding and function of the transcription factor Pho4. Mol Cell 42, 826–836.